Chapter 4
Timber-Glass Prefabricated Buildings

Abstract This chapter is based on using timber and glass which were formerly rather neglected as construction materials. With suitable technological development and appropriate use, they are nowadays becoming essential construction materials as far as energy efficiency is concerned. Their combined use is extremely complicated, from the energy efficiency perspective presented in Sect. 4.3 on the one hand and from the structural viewpoint presented in Sect. 4.4 on the other, which sets multiple traps for designers. A good knowledge of their advantages and drawbacks is thus vitally important, as will be seen in the first two sections of the current chapter. The results of the comparative analysis contained in the last two sections can serve as a good frame of reference to architects and civil engineers in their approximate estimation of the energy demands emerging from different positions and proportions of the glazing surfaces, in addition to being of assistance in their assessment of the influence of the building shape exerts on the energy demand of prefabricated timber-frame buildings.

4.1 The History of Glass Use

The origins of glass manufacture are still uncertain. Historical sources and archaeological evidence trace them to Mesopotamia or Ancient Egypt. In general, the first glass-made objects (where glass was used as an independent material) appeared no sooner than around 3,000 BC [1] and were mainly meant as decoration. Manufacturing glass vessels and other useful items began only much later.

In the second century BC, the Phoenicians made a revolutionary discovery of glass blowing which permitted limitless ways of glass-shaping. A major turning point in the development of glassmaking goes back to the times of the Roman Empire and the Romans who were the first manufacturers of clear glass. Glass-blowing as a glass-forming technique of Syrian origin replaced the old Roman glassmaking techniques.

V. Žegarac Leskovar and M. Premrov, *Energy-Efficient Timber-Glass Houses*, Green Energy and Technology, DOI: 10.1007/978-1-4471-5511-9_4,

The Romans began using glass for architectural purposes and introduced the first instances of the glazing in the exterior wall openings. The spreading of the glassmaking technique reached also northern Alpine regions and after the collapse of the Western Roman Empire it continued to develop in the near east and the world of Islam. The seventh century witnessed a discovery of a simple and inexpensive window glassmaking method, whereas the eighth century saw the appearance of coloured glass which was later used for stained glass windows in churches. From the fifteenth to the seventeenth century, glassmaking continued its development in the Venetian Republic which remained a glass-manufacturing centre until the eighteenth century. In the sixteenth century, the production of glass stretched further over European countries among which Bohemia distinguished itself by making a most intense headway in the field of glass manufacturing. Two of the most important hand-blown window glass production techniques dating from the early Middle Ages included the cylinder blown sheet and the crown glass. Both remained basic glass-manufacturing methods until the late nineteenth and the early twentieth centuries [2].

The flourishing of the glass-manufacturing industry was marked by technological advances. Innovative procedures of glassmaking kept emerging since 1687 when a Frenchman, Perrot introduced the cast glass process which enabled the production of glass panes in the size of 1.2×2.0 m. Glass became an item of mass production only towards the end of the Industrial Revolution. In 1839, the Chance brothers improved the process of making cylinder blown sheet glass. Further innovations were Siemens' patent of the melting furnace in 1856, followed by Lubbers' development of the mechanical process to combine blowing and drawing, appearing at the end of the nineteenth century, and by Owen's invention of the machine for blowing of bottles, dating from the same period. A key person and a father of modern research of glass was F.O. Schott, a German chemist and scientist whose scientific work conducted in the late nineteenth century involved methods for studying the effects of various chemical elements have on optical and thermal properties of glass. Other important improvements in glass production that followed in the twentieth century were the 1913 Fourcault process of drawing glass panes directly from the molten glass and the Libbey-Owens process, a similar method developed by Colburn, which enabled production of 2.5-metre-long glass panes of different thicknesses depending on the speed of the drawing. Combining both of the methods resulted in a process applied by the Pittsburgh Plate Glass Company in 1928, which led to an increase in the manufacturing speed. In 1919, the improved cast glass process invented by Bicheroux allowed the production of panes in the size of 3.0×6.0 m. However, one of the most important innovations was the 1950' Pilkington float-glass process which has been the basis of glass production until the present times [2].

Another milestone in the beginnings of modern glass construction was set by the development of skeletal iron construction. Both provided a technical basis for the erection of the first glazed load-bearing structures in the early nineteenth century, known as the English greenhouses. Stability of such delicate free-standing

enclosures with domed and folded glazed roofs was achieved mainly with the bracing provided by small glass shingles embedded in the putty [3]. The progress in glass technology, which allowed the production of larger glass panes, led to the use of glass for covering purposes while its construction-related significance was almost completely lost. Throughout the twentieth century, the visual potential of glass was strongly emphasized through the phenomenon of transparent architecture focusing on large glass façades. The latter had a positive impact on daylight conditions and the aesthetic perception of internal spaces open to the exterior, while at the same time, the indoor living climate in buildings with large glazing areas was not a matter of high thermal comfort any more. Single-pane glazing used at that time caused large heat losses in winter in addition to unpleasant summer period heat gains resulting in overheating. A dynamic evolution of the glazing in the last 40 years has resulted in insulating glass products with highly improved physical features suitable for application in contemporary energy-efficient buildings.

An ongoing driving force of the development leads to the conclusion that glass as an important building material will not cease to be used in the future owing to its remarkable properties and multiple options of usage which have not yet been surpassed by any other material.

4.2 Glass as a Building Material

Glass can nowadays be treated as a dominating material in modern architecture. Not only its optical appearance but also its numerous technical functions classify glass as an indispensable building design component providing protection against atmospheric influences, natural lighting, energy storage and generation, etc. The energy aspect of this building material was often treated as a weak point in the past, whereas in the last few decades, it has become one of the main drivers of technical development of glass for the purposes of the building industry. Another important novelty arising from the phenomenon of increasing the size of glazing surfaces in modern buildings is taking the load-bearing function of glass into account, where its integration with other building materials plays a vital role.

Glass is an amorphous form of matter. Although different explanations about whether glass should be classified as a solid or as a liquid might have appeared over a time, it is important to define glass as a solid material, i.e., a solidified liquid.

The idea that glass is a liquid came from observing window glass in old churches. The glass being thicker at the bottom than at the top gives an impression as if the gravity had caused the glass to flow towards the bottom over several centuries, which in fact is not true. The difference in thickness arises from an ancient technique of the crown glass process, where glass sheets were thicker towards the edges.

Table 4.1 Chemical composition of predominantly used glass types

Substances	Chemical symbol	Share of substance in glass (%)
Silicon oxide	SiO_2	69–74
Calcium oxide	CaO	5–12
Sodium oxide	Na_2O	12–16
Magnesium oxide	MgO	0–6
Aluminium oxide	Al_2O_3	0–3

Glass is formed when the liquid is rapidly cooled from its molten state through its glass-transition temperature (T_g) into a solid state without crystallization [4]. Since the molecules of glass follow a completely random order and do not form a crystal lattice [5], its configuration is geometrically irregular, which gives glass its transparency. Upon heating, glass gradually changes from a solid to a plastic–viscous and finally to a liquid state. In comparison with timber, whose properties depend strongly on the direction of the grain, glass exhibits amorphous isotropy, i.e., its properties are uniform regardless of the direction of measurement.

Nowadays, the building industry predominantly uses soda-lime-silica glass (SLS). It consists of an irregular three-dimensional network where each silicon (Si) atom is bounded to four oxygen (O) atoms. The making of SLS involves four phases, i.e., preparation of raw material (soda ash, lime, silica sand and cullet), melting in a furnace, forming and finishing. Apart from float glass, which is generally used for windows, other products resulting from the above-described manufacturing process are container glass, pressed and blown glass. The composition of predominantly used glass types is presented in Table 4.1.

Apart from the basic substances, glass contains also small proportions of other substances, e.g., magnesium oxide and aluminium oxide, which provide additional influence on its colour and physical properties. Among the latter, the thermal conductivity (λ), the specific heat capacity (c), the transition temperature (T_g) as well as the average reflective index in the visible range of wavelengths (n) are of primary interest from the energy viewpoint of our further research. General physical properties of soda-lime-silica glass are presented in Table 4.2.

The thermal conductivity of soda-lime-silica glass is comparable to that of concrete whose value also ranges from 0.5 to 1.5 W/mK. The density and the coefficient of thermal expansion values of the two materials (c.f. Table 4.3) prove

Table 4.2 General physical properties of soda–lime–silica glass

Property	Symbol with units	Value
Transition temperature	T_g [°C]	564
Liquid temperature	T_l [°C]	1,000
Density	ρ [kg/m^3]	2,500
Coefficient of thermal expansion	α_T [K^{-1}]	0.9×10^{-5}
Thermal conductivity	λ [W/(m K]	1.0
Specific heat capacity	c [J/(kg K]	720
Average reflective index in the visible range of wavelengths	n	1.5

Table 4.3 Mechanical characteristics of float glass, softwood and steel

	Density ρ [kg/m^3]	Compress strength f_c [N/mm^2]	Tensile bending strength f_{mt} [N/mm^2]	Modulus of elasticity E [N/mm^2]	Coefficient of thermal expansion α_T [10^{-5} K^{-1}]
Float glass	2,500.00	800.00	45.00	70,000.00	0.90
Timber C30	460.00	23.00	30.00	12,000.00	0.50
Steel S240	7,850.00	240.00	240.00	210,000.00	1.20
Concrete C30/37	2,500.00	30.00	2.9	33,000.00	1.00
Ratio glass/timber	5.43	34.78	1.50	5.83	1.80
Ratio glass/steel	0.32	3.33	0.18	0.33	0.75
Ratio glass/concrete	1.00	26.67	15.52	2.12	0.90

to be a further similarity in addition to the relationship between the compressive and the tensile strengths (which will be further discussed in Sect. 4.2.1), with the compressive strength of both materials being very high and their tensile strength essentially lower. We can therefore presume that the behaviour of glass in many physical aspects demonstrates closely similar characteristics to those of concrete.

4.2.1 Structural Glass

Glass is a molecularly cooled liquid that the final stage of production turns into a solid. Owing to its optical and energy related, i.e., insulating properties, glass has become an ever more widely used material of the last decade and is no longer solely responsible for daylighting or the transparency of the building. Furthermore, its improved strength properties enabled the use of large glazing areas as additional structural resisting elements. Even though structural problems related to certain mechanical disadvantages of glass still exist, they can be generally avoided if glass elements are properly incorporated in the structural system of the building.

One of the main drawbacks of glass used as a load-bearing material lies in its being a relatively *brittle material* with mostly a significantly low degree of post-cracking resistance (Fig. 4.1a, b). When compared to the stress–strain diagram for timber in compression parallel to the grain (Fig. 3.8) and to that of timber in tension parallel to the grain (Fig. 3.11), glass demonstrates considerably lower ductility. As a consequence, resisting problems can occur in glass elements located in heavy seismic or windy areas. Post-cracking behaviour of glass depends on the type of glass, which is a matter of further discussion.

On the other hand, glass has a high *modulus of elasticity* of approximately 70 GPa, which is a value about 6 times higher than that of softwood in the grain

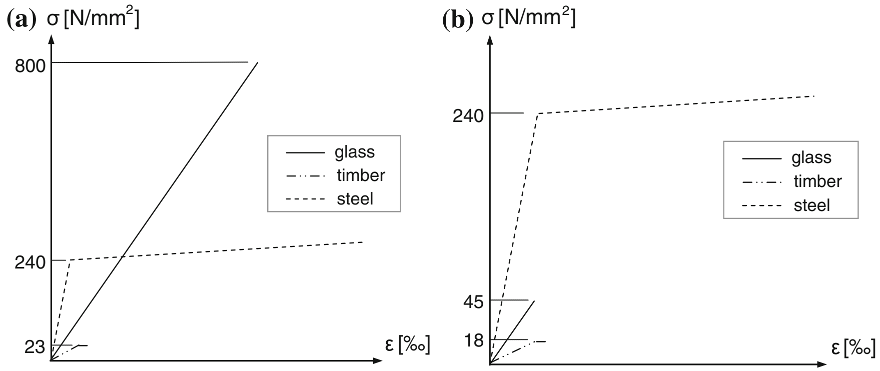

Fig. 4.1 σ–ε diagram of glass, timber and steel in compression (**a**), and tension (**b**)

direction, although 3 times lower than that of steel and equal to that of aluminium. Thus, we can claim that glass is relatively stiff material and that properly inserted glass elements can significantly contribute to the stiffness of the structure. A difficulty still remaining is seen in the behaviour of glass, which is almost linear-elastic until failure.

The *strength* of glass strongly depends on the type of loading. The strength of glass in compression is extremely high, mostly ranging from 700 to 900 MPa, which is about 2 times higher than in the case of steel and about of 40 times higher than the strength of timber. The tensile bending strength depends on the type of glass, but varies mostly from 45 MPa for float glass to 150 MPa for chemically strengthened glass. Both values prove to be far above those of the tensile strength of timber, but they are on the other hand far under those measured in steel.

Since most of the glass areas are placed in the south façade of the buildings and therefore subjected to a very high temperature effect, especially in the summer period, the *coefficient of thermal expansion* α_T is of vital importance, when glass and timber are used as composite elements. The values of α_T for glass, softwood and hardwood are 0.9×10^{-5}, 0.5×10^{-5} and 0.8×10^{-5} K^{-1}, respectively. Enlarged shear stresses may therefore occur in the adhesives between timber and glass elements when these are subjected to a heavy temperature effect.

Table 4.3 shows the most important mechanical values of float glass. They are compared to the values of softwood, concrete and steel.

It is obvious from the glass/timber, glass/steel and glass/concrete calculated ratios that two of the glass properties demonstrate substantial deviation from the density ratio of all four materials, namely the compressive strength of the glass which is extremely high and its tensile bending strength which is extremely low. The relationship of the values of the elasticity modulus is in good accordance with the relationship of the densities. The stress–strain diagrams (σ-ε) for glass, steel and timber are presented in Fig. 4.1a, b for the compression and tension, respectively. The linear simplification for timber is made according to the σ-ε diagram for compression in Fig. 3.8 and the σ-ε diagram for tension in Fig. 3.11.

There are many different types of structural glass:

- Float glass
- Annealed glass
- Heat-strengthened (partially tempered) glass
- Fully tempered (toughened) glass
- Chemically strengthened glass
- Laminated glass.

Float glass is produced by pouring molten glass onto a bed of molten tin by the process invented by Sir Pilkington in 1953. The glass floats on the tin and levels out as it spreads along the bath, giving a smooth face to both sides although the two sides of a glass sheet tend to be slightly different. Due to its molecular structure, the behaviour of glass is perfectly elastic until failure and there are no plastic deformations before the appearance of the first cracks in the structure. Float glass is produced in standard metric nominal thicknesses of 2, 3, 4, 5, 6, 8, 10, 12, 15, 19 and 25 mm in jumbo sheet stock sizes of 3.21 $\times$ 6 m [4]. Oversized jumbo sheets for the glass market are produced to a limited extent. For special purposes, some glass factories produce sheets up to 12 m in length [3]. Float glass is the most widely used type of glass today.

Annealed glass is basically float glass produced by a cooling process slow enough to avoid internal stresses caused by heat treatment in the glass. Glass can be made more load resistant by inducing the compressive stresses on the surface. It becomes annealed if heated above the transition point and then allowed to cool slowly. If glass is not annealed, it will retain many of the thermal stresses caused by quenching and will sustain a significant decrease in its overall strength [4]. Annealed glass is very brittle and breaks into large pieces (Fig. 4.2) which can cause serious injuries sustained by people being close to such glazing surfaces. Therefore, certain codes do not allow the use of annealed glass in areas where a

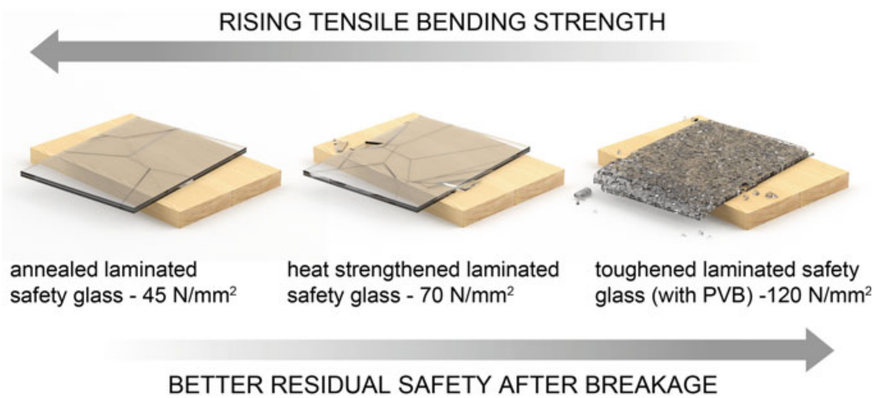

Fig. 4.2 Standard laminated glass types with their corresponding breakage forms and the tensile bending strength, adopted from Močibob [4]

risk of such injuries exists. Annealed glass has the lowest mechanical strength of all modern basic structural types of glass presented in this subsection.

Heat-strengthened (partially tempered) glass is the most common type of strengthened glass used in structural resisting elements. It has a thickness of less than 12 mm and has been tempered to induce surface residual stresses, but at a lower temperature and with a lower cooling rate than fully tempered glass. Hence, the name partially tempered glass. It differs from fully tempered glass in having lower residual stresses and breaking into evidently larger pieces, but still smaller ones than in the case of annealed glass (Fig. 4.2). Its tensile bending strength is halfway between the annealed (45 N/mm^2) and the fully tempered glass strength (120 N/mm^2), ranging at about 70 N/mm^2.

Fully tempered (toughened) glass is made from annealed glass by a thermal tempering process patented by R.A. Seiden. The process of manufacturing starts with glass being placed onto a roller table which takes it through a furnace that heats the glass to above its transition temperature. The glass is then rapidly cooled with draughts of air in a manner that lets the inner portion of the glass remain free to flow for a short time [4]. Fully tempered glass must be cut to the size and pressed to the shape before tempering, since glass once tempered cannot be reworked. This type of glass is referred to as safety glass because it breaks into small cuboid pieces, as opposed to ordinary annealed glass (Fig. 4.2), and reduces the risk of injuries caused by the breaking of glass panes. Toughened glass has consequently gained popularity in structural design. Its advantages taken from the structural point of view lie in the tensile bending strength reaching up to 120 N/mm^2, which is almost triple the value measured in ordinary annealed glass.

Chemically strengthened glass is a result of a process of strengthening by submerging glass into a bath containing a potassium salt or potassium nitrate heated to 450 °C. This causes sodium ions in the glass surface to be replaced by the larger potassium ions from the bath. Consequently, the potassium ions block the gaps left by the smaller sodium ions when these migrate to the potassium nitrate [4]. In contrast to fully tempered glass, chemically strengthened glass can be cut after the manufacturing process, but it losses the obtained additional strength within the area of about 20 mm from the cutting zone. Chemically strengthened glass cannot be classified as a safety glass because it breaks into long pointed pieces, similarly as annealed glass, and must be therefore laminated when applied in buildings. On the other hand, owing to chemical strengthening, the increased tensile bending strength of this type of glass is the highest and can reach the value of even 150 N/mm^2.

Laminated glass is not considered as a glass type but can be treated as a glass product composed of glass sheets glued together in a manner to improve the residual load-bearing capacity of glass panes. It was patented in 1903 by a French chemist, Eduard Benedictus. Laminated glass can be composed of annealed, partially tempered, fully tempered or even chemically strengthened glass sheets (Fig. 4.2). The majority of mechanical properties of laminated glass depend on the glass type of the sheets glued together with a transparent interlayer whose thickness is usually a multiple of 0.38 mm. The most commonly used interlayer is

polyvinyl butyral (PVB), followed by cast-in-place resin (CIP), ethylene vinyl acetate (EVA) and SentryGlas Plus (SGP). Upon breaking of glass sheets, the interlayer holds the glass pieces together and assures a certain level of post-breakage resistance of the panes in addition to protecting the glass element against total collapse. As a result, laminated glass remains glued to the foil when shattered and has an increased residual load-bearing capacity. It is therefore used to ensure the resistance after breakage in areas submitted to a possible human impact, where glass could fall if shattered [4]. Specialist glass-processing companies are able to laminate single and multi-layer laminated sheets up to a jumbo panel size of 3.21×6 m, in exceptional cases even up to 7 m in length [3].

Breakage forms of the described standard glass types can be observed in Fig. 4.2. All structural glass types are presented as laminated glass products whose pieces are kept together on PVB after breakage. The level of safety, meant as a breakage form according to the size of the pieces, increases with the degree of strengthening, which is also true of the tensile bending strength whose values mount from 45 to 120 N/mm^2. Other mechanical properties, such as the compressive strength, the modulus of elasticity and the coefficient of thermal expansion, remain constant and do not depend on the strengthening of glass. The values for float glass given in Table 4.3 can be consequently adapted to all the presented types of structural glass.

4.2.2 Adhesives

The function of adhesives in timber-glass composites is to bind the two resisting materials—timber and glass whose mechanical properties show significant differences (c.f. Table 4.3 and Fig. 4.1). Glass is a very brittle material with practically no post-breakage capacity as opposed to timber which is more a ductile, but a very flexible material having a very low modulus of elasticity. It is consequently of utmost importance for adhesives to assure resistance and a high range of ductility of such composed load-bearing elements, simultaneously to finding balance between strength and deformability. Adhesives must also allow for expansion and shrinkage of timber, according to loading and humidity variations [6].

According to [7], adhesives used in timber-glass composites can be classified into three groups:

- Highly resistant and insufficiently flexible adhesives—rigid adhesives (acrylate, epoxy)
- Highly flexible adhesives, yet insufficiently resistant to loading—elastic adhesives (silicone)
- Adhesives that balance both key factors—strength and flexibility—semi-rigid adhesives (polyurethane, superflex polymers).

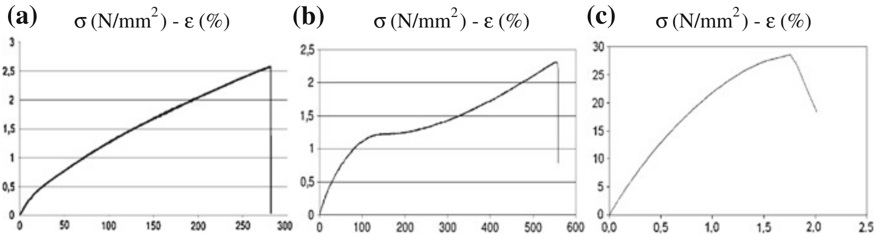

Fig. 4.3 σ-ε diagrams of different types of adhesives in tension; **a** silicone, **b** polyurethane, **c** epoxy

Stress–strain (σ-ε) diagrams in tension of all three basic adhesives types are schematically presented in Fig. 4.3.

The above diagrams obtained through short-term tests show an essentially higher strength of epoxy in comparison with polyurethane or silicone. What is more, the strains in epoxy can be even 100 times lower than those in silicone or polyurethane, which needs to be considered when deciding on the type of adhesive. Since we usually deal with the mid-term and long-term loads in practice, we ought to draw attention to findings by Haldimann et al. [8] who proved that the long-term strength of silicone is only about 10 % of its short-term strength due to a highly creep behaviour of silicone sealants. Other findings deserving to be mentioned are those by Cruz et al. [7], obtained from the shear tests results showing that the failure mode of timber-glass elements depends on the strength of the adhesive. It can be generally observed that glass regularly collapses in combination with high-resistance adhesives.

A further matter of importance is strong dependence of the optimal thickness of the bond line between timber and glass on the strength of the adhesive. The thickness of elastic adhesives is approximately 3 to 4 mm, while that of rigid adhesives ranges only from 0.3 to 0.5 mm. Figure 4.4 demonstrates strength behaviour of both adhesive types in dependence on the thickness of the bond line.

The main advantages and disadvantages of the above-mentioned adhesives used in timber-glass applications are thoroughly discussed in different studies, e.g., in Blyberg et al. [9] and Blyberg [10]. As seen in Fig. 4.4a, b, the results of the adhesive testing made within the above-listed studies showed that acrylate and polyurethane adhesives had significantly higher strength than silicone adhesives. Acrylate has a glass-transition temperature of 52 °C, which means that the properties of acrylate adhesives may undergo a substantial change when the temperature is increased. Winter et al. [11] claim that acrylates exhibit a dramatic reduction in strength when exposed to temperatures above 50 °C or to extreme humidity (RH). On the other hand, a study by Blyberg [10] on the effect humidity has on the acrylate adhesive bond did not indicate any huge effects on the strength of specimens kept at 85 % RH, which is a humidity level expected within indoor climate conditions.

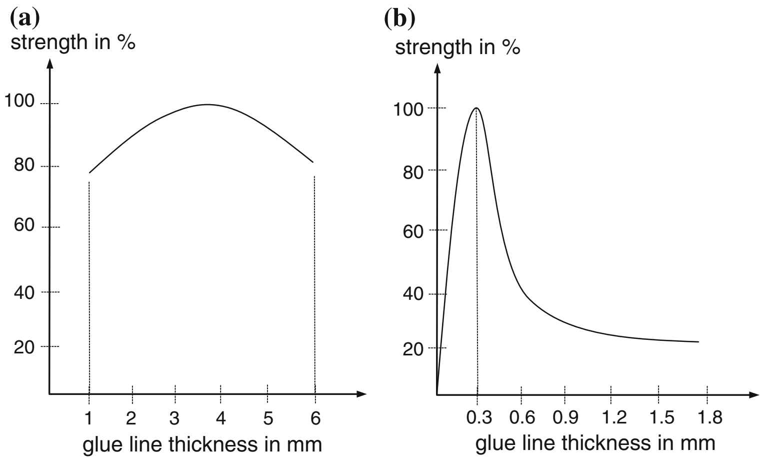

Fig. 4.4 Strength of elastic (**a**), and rigid (**b**) adhesives in dependence on the glue line thickness

Pequeno and Cruz [12] conducted a meticulous analysis of three different adhesives types (silicone, polyurethane and polymer), with respect to a number of structural and aesthetic aspects. The silicone adhesive proved to be the most advisable, as it allows for greater indexes of flexibility and assures the needed structural mechanical resistance. Moreover, silicone showed the highest UV resistance which is an utterly important fact to be taken into account when installing glazing surfaces in south-oriented façades, in view of highest possible degree of solar gains.

4.2.3 Insulating Glass

In order to understand the main functions of insulating glass and compare different glazing structures, basic knowledge of building physics is required.

4.2.3.1 Transmission of Solar Radiation Through Glazing

As solar radiation hits the glass panes, it is partly reflected, partly absorbed and partly transmitted directly through the glass. The absorbed radiation heats up the glass panes and is later emitted to the interior and exterior through heat radiation and convection (Fig. 4.5).

Figure 4.5 clearly shows that the total transmitted solar energy consists of directly transmitted solar radiation and of radiation absorbed in the glass panes and transformed into heat which is later emitted to the interior. The amount of total transmitted solar energy is expressed by the value of g, the coefficient of permeability of the total solar radiation.

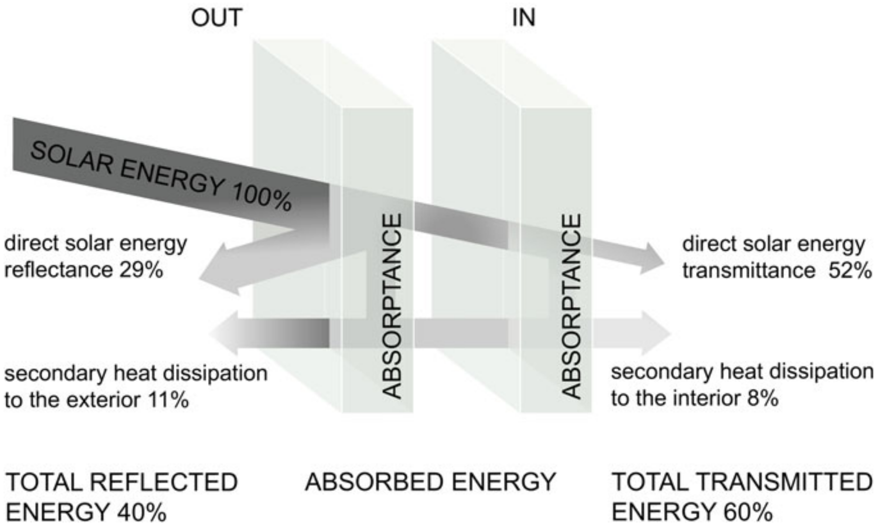

Fig. 4.5 Scheme of solar energy flow through an insulating glass unit

The concept of energy-efficient building design attributes a vital role to solar radiation, i.e., to solar gains through the transparent building envelope. Due to their solar radiation permeability, windows can contribute to the energy balance of buildings. On the other hand, widows represent areas in the building envelope with the highest heat loss potential, since the average *U*-value of windows is generally higher than the average *U*-value of opaque building elements (walls, ground slab and roof). However, constant development of the insulating glass technology results in launching ever new products with multiple gas-filled chambers and different coatings which substantially contribute to the reduction in heat losses through glass panes.

How is heat transferred through the insulating glass unit and what is the amount of heat flow influenced by? Heat transfer through a window occurs via three main mechanisms; conduction, convection and radiation (Fig. 4.6).

Conduction heat flow is transferred through adjacent atoms and molecules of gasses or solids. Heat always transfers from the warmer to the cooler side of a window, which means that the direction of conductive heat flow may change in the course of a day, month or year. Conduction heat flow occurs through the glass panes, the edge seal or spacer bar, the frame and even through the air or inert gas in the pane interspace. It can be minimized by adding glass panes, by using low-conductivity gasses, spacers with thermal brake and frames made of low-conductivity materials. Convection heat flow is the transport of heat away from the surface caused by air movement. It occurs in the pane interspaces and on each external side of the window. The use of inert gasses in the pane interspaces reduces energy losses due to convection. Radiation is a thermal exchange between the surface and the surrounding and always moves from a warmer surface to the cooler

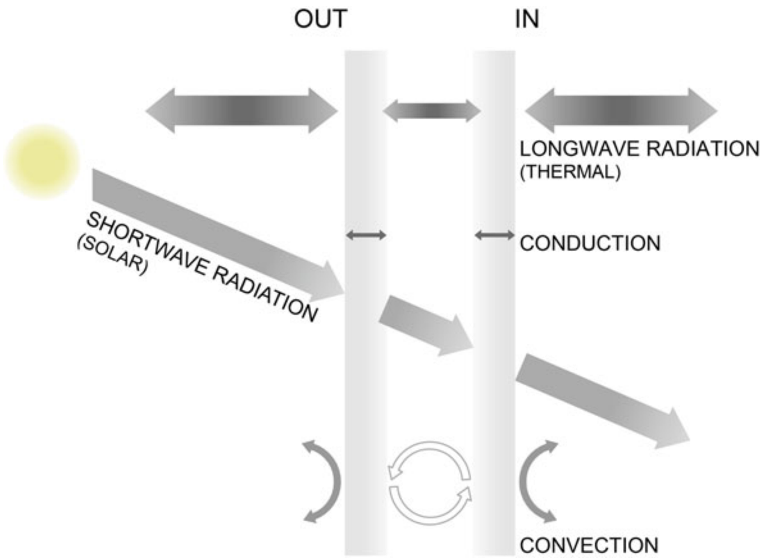

Fig. 4.6 Mechanism of heat transfer through the insulating glass unit

surrounding. Heat is usually radiated from the surface of the heated elements into the air and absorbed by glass to be reradiated afterwards to the interior or exterior. Radiation heat losses can be reduced by the use of low-emissive coatings applied to the glass panes.

The official definition of "insulating glass" is determined in EN 1279-1 [60] as "Multiple-pane insulation glass is a mechanically stable and durable unit comprising minimum two glass panes that are separated from each other by one or more spacing elements and are hermetically sealed at the edges". A standard insulating glass unit consists of two or three panes, while a high-efficiency insulating glass unit consists of four or even more glass panes.

4.2.3.2 Energy Indicators of Insulating Glass Units

A contemporary insulating window element consists of a glazing unit and window frame. The energy performance of windows can be expressed by two general indicators:

- The coefficient of thermal transmittance U [W/m^{2}K] with separate values for the glazing, the frame and the entire window element. It indicates the amount of heat of passing through 1 m^2 of component per unit of time based on a temperature difference of 1 K
- The coefficient of permeability of the total solar energy g [% or values 0–1] of the glazing. It indicates the sum of solar energy transmitted directly through the

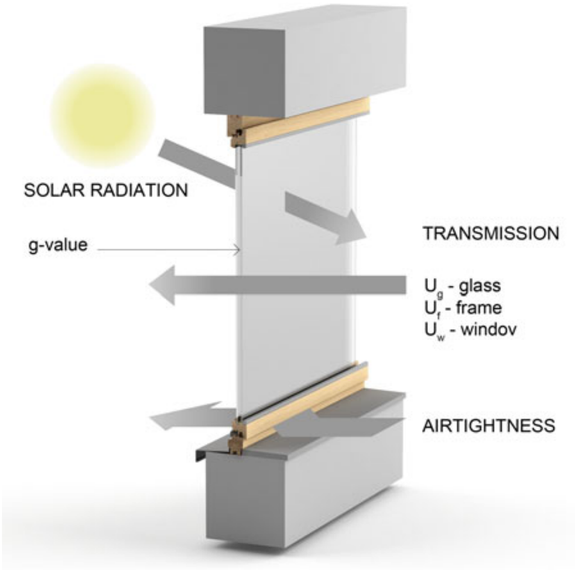

Fig. 4.7 Main indicators of the energy efficiency of windows

glass and solar energy absorbed in the glass panes and later emitted to the interior.

Besides the above-listed indicators, proper airtight installation plays a vital part in the energy-efficient performance of windows, since it significantly reduces infiltration causing ventilation heat losses (Fig. 4.7).

Glazing properties exert influence not only on the building's thermal performance but also on the quality of the interior daylight. Sufficient amount of visible radiation transmitted through the glazing reduces the need for artificial lighting, which saves electrical energy. Indicators expressing the quantity of transmitted and reflected light are the following:

- The light transmission coefficient LT [%], expressing the percentage of visible solar radiation (wavelength from 380 to 780 nm) transmitted through glass.
- The light reflection coefficient *R* [%], expressing the percentage of visible solar radiation (wavelength from 380 to 780 nm) reflected by glass.
- Additional indicators showing the quality or quantity of transmitted solar energy are as follows:
- Colour rendition index *Ra* [0–100], indicating colour recognition in the interior and colour recognition through the glazing itself. The highest value of 99 indicates neutral colour recognition.
- The selectivity factor $S = \mathrm{LT}/g$, representing the ratio between light transmittance LT and the degree of total solar energy permeability g. A higher S-value expresses a better ratio.

- The shading coefficient Sc = $g/0.80$ indicates the mean transition of solar energy related to the degree of total solar energy transmittance of an uncoated two-pane insulated glass unit. This indicator is essential for calculating the required cooling load of the building [UNIGLAS® [13]].

In addition to the main indicators expressed above, glass producers use a number of other indicators to provide accurate description of their products, i.e., of the quantity or quality of the solar energy absorbed, transmitted or reflected by the glass panes.

4.2.3.3 Parameters Influencing Energy Properties of Insulating Glass

A window is treated as a complex element with its overall coefficient of thermal transmittance (U_w) depending not only on the glazing but also on the type of window frame and spacer element. The U_w can be read or measured or calculated. Determination by means of calculation is based on the following equation according to ISO EN 10077-1:2006 [14]:

$$U_w = \frac{A_g \cdot U_g + A_f \cdot U_f + l_g \cdot \psi}{A_g + A_f} \tag{4.1}$$

with the following quantities presented in Fig. 4.8:

U_w The heat transfer coefficient of the window,
U_f The heat transfer coefficient of the frame,
U_g The heat transfer coefficient of the glazing,
A_f The area of the frame,
A_g The area of glass,
l_g The length of the glazing perimeter,
ψ Linear heat transmittance of the glass edge (describes thermal bridges of a constructional component).

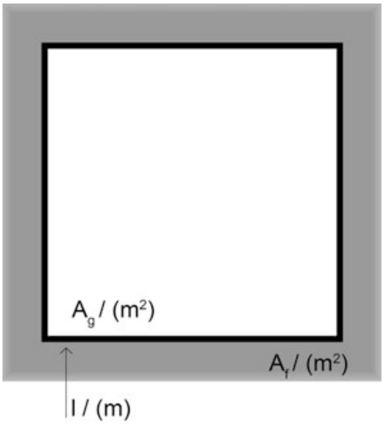

Fig. 4.8 Areas of the insulating window considered in calculation of the U_w

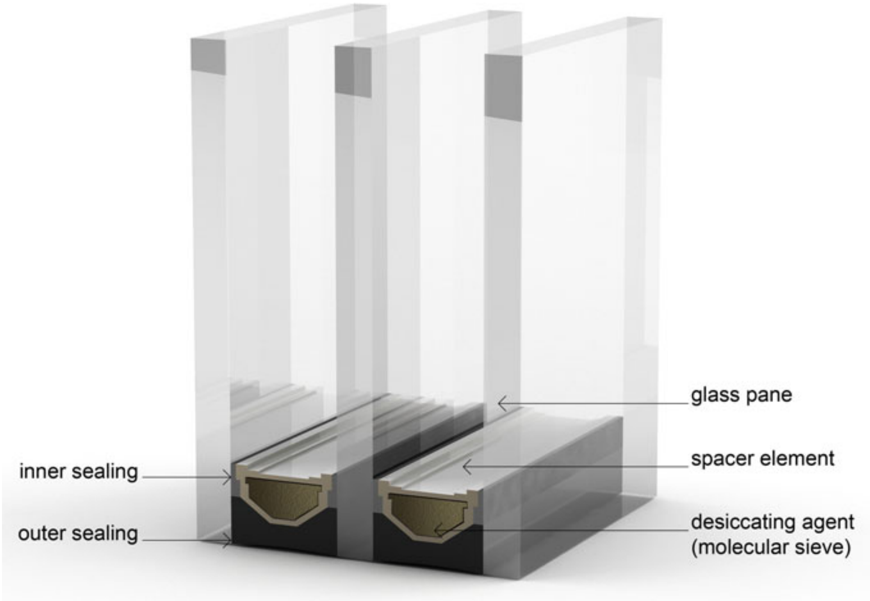

Fig. 4.9 Composition of a typical three-pane insulating glass unit

Thermal transmittance (U_g) of the glazing depends on the number and dimension of the pane interspaces, on the type of gas filling, on the number, type and emissivity of the heat insulation layers, i.e., glass coatings, and on the type of edge seal and spacer element. The composition of a three-pane insulating glass unit is presented in Fig. 4.9.

Number of Glass Interspaces

Increasing the number of glass panes and pane interspaces results in the reduction in heat flow and light transmittance.

Glass Coatings

A major part of the energy loss in an insulating glass unit is caused by radiation, while in a window frame, the main energy loss is due to conduction. As a consequence, different parts of the window require different approaches to energy loss reduction. In the area of glazing, the main energy loss reduction strategy should therefore focus on preventing heat to radiate from the interior to the exterior.

The above-mentioned heat radiation prevention can be achieved by using glass coatings, i.e., thin metal and metal oxide layers which are applied to the glass surface either by the pyrolytic or the magnetronic method with a purpose of reducing the permeability of radiation through the glass panes. It depends on the selectivity of the coating whether the latter reduces short-wave solar radiation (solar coatings) or long-wave heat radiation (heat coatings or low-e coatings). In the pyrolytic method, molten metal or metal oxide is applied to glass at high temperatures by either dipping or spraying, which results in a hard coating. Magnetronic sputtering is a process of applying thin layers of various metal and metal oxide coatings to glass as soft coatings. A wide range of light reflection, light transmission, infrared reflection and colour options of the glass surface are thus permitted. Magnetronic sputtering also allows for a combination of heat and solar coatings to be applied—one on top of the other [15].

Individual layers of heat coatings (also called low emissivity or low-e coatings) are invisible and act as selective filters which are permeable to the short-wave solar radiation of a wave length up to 2,500 nm, but impermeable to the long-wave heat radiation, especially the long-wave IR radiation of the wave lengths ranging from 3,000 to 50,000 nm. As seen from a practical viewpoint, solar radiation can pass through the glass into the room where it is absorbed by the surfaces of the interior which warm up and later emit the energy as the long-wave IR radiation. Heat coatings applied to glass act as impermeable to the IR long-wave heat radiation by reflecting the radiation back to the room. Low-e coatings are usually applied to the glass pane adjacent to the interior to the side facing the cavity or potentially to both outer panes to the sides facing the cavity. The panes' surfaces are normally numbered from the outside to the inside (Fig. 4.10), which helps describing the position of individual coatings. Application of low-e coatings reduces the U_g-value.

Solar coatings reduce the permeability of short-wave solar radiation through the glass panes, which results in the lower g-value for glass. The extent to which the

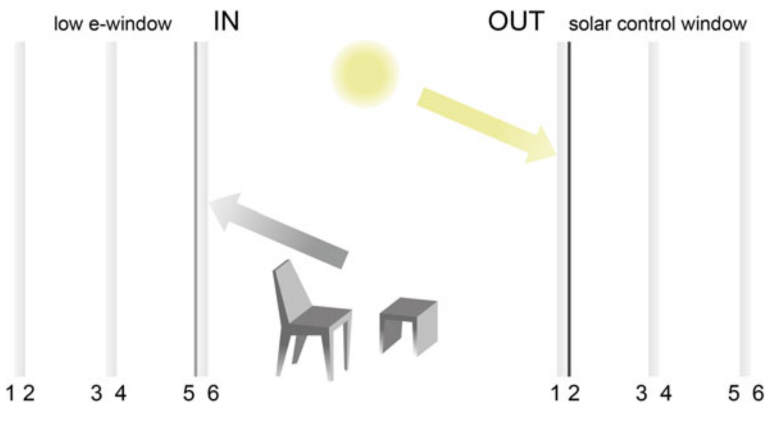

Fig. 4.10 Basic principle of positioning the coatings in the insulating glass unit

g-value and the light transmittance of glass are reduced depends on the ratio of selectivity of the solar coating. Almost all solar coatings, with the exception of soft coatings reduce both, the permeability of solar energy and the light transmittance. Solar coatings are usually applied to the outer pane adjacent to the exterior to the side facing the cavity. Some hard coatings can be applied to the external side of the outer glass pane (position 2 in Fig. 4.10), since they are resistant to environmental conditions. It is also possible to apply a combination of both, solar and low-e coatings on a single-glazing pane.

Where and why do we use solar coatings? In residential buildings, the strategy of passive solar design usually refers to exploitation of solar energy transmitted through transparent surfaces in order to reduce the energy demand for heating. On the other hand, there exists a risk of overheating in the summer period, which can be prevented by the use of appropriate shading elements. The use of solar coatings for the glazing in residential buildings is not advisable, since it has a negative impact on the principle of solar energy use and the quality of daylight. There are nevertheless some exceptions in residential architecture, e.g., large winter gardens, pavilions, glazed swimming pools, where the prevention of summer overheating is more important than the solar energy gain in winter. In the architecture of public, office and administration buildings, a permanent trend heading towards transparency requires large glazing surfaces. Since the use of external shading elements is not always appropriate in such public buildings, the use of sun protective coatings reduces overheating of the rooms by means of reflection and absorption of solar energy and a consequent reduction in the load on air conditioning systems in buildings.

Number of Glass Interspaces and Cavity Fillings

Increasing the number of glass panes and pane interspaces causes the reduction in heat flow and light transmittance. The glazing interspace in a standard insulating glass unit is usually 12–16 mm wide and filled with a rare gas in order to reduce thermal conductivity. The gas used in most cases is argon or krypton. The influence of the type of cavity gas of the number of pane interspaces and low-emissive coatings on the U_g-value is presented in Table 4.4. The data are based on the review of Gustavsen et al. [16].

Table 4.4 Typical U_g-values for different configurations of the window glazing

Glazing U_g-value [W/m^{2}K]				
Glazing configuration [mm]	Cavity gas			
	Air	Argon	Krypton	
No coating	4	5.8	–	–
	4-12-4	2.9	2.7	2.6
	4-12-4-12-4	2.0	1.9	1.7
Low-emissive coating	4-12-E4	1.6	1.3	1.1
	4-12-4-12-E4	1.3	1.0	0.8
	4E-12-4-12-E4	1.0	0.7	0.5

According to the above data, application of multiple interspaces, gas fillings and coatings into the configuration of a glass unit reduces the U_g. Data based on the review of Gustavsen et al. [16] show that a 4 mm pane of float glass has a U_g of approximately 5.8 W/m^{2}K. A double-pane insulating unit without coatings filled with argon has a U-value of approximately 2.7 W/m^{2}K. Adding a single low-emissive coating leads to a reduction in U_g which then attains a value of 1.3 W/m^{2}K. In a triple-glazing unit, filled with argon and coated on both external panes, the U_g is about 0.7 W/m^{2}K, while if filled with Krypton, the U_g-value approximates 0.5 W/m^{2}K. Insulating glazing units currently under development are made of multiple chambers with different coatings and gas-filled cavities whose values range around $U_w = 0.30$ W/m^{2}K, which is relatively close to the U-value of external walls prescribed for low-energy houses ($U = 0.20$ W/m^{2}K).

Spacer

Spacer is an element that holds the panes in an insulating glass unit at the appropriate distance. To prevent condensation in the pane interspaces, the spacer is filled with a desiccating agent, which can absorb any penetrating moisture. In addition, it has to assure the sealing of the air- or gas-filled pane interspace which is made of two seals, a primary seal between the spacer profile and the glass and the secondary seal applied to the external side of the spacer bar. Many different types of spacers can be currently found on the market. The weakness of the standard aluminium spacers is their high conductivity resulting in a large thermal bridge causing the cold edge effect in the edge area of the insulating glass unit, which increases a risk of condensation. The market nowadays offers several innovative edge seal types with lower conductivity and interrupted thermal bridging in the edge area (warm edge effect), which improves the U-value of the entire insulating glass unit and significantly contributes to the increase in the interior surface temperature at window edges. Such edge seals include thermally broken aluminium or stainless steel spacers, silicone foam spacers, corrugated metal spacers, fiberglass spacers, PVC spacers, etc. Gustavsen et al. [16]. With the increasing use of high-insulating windows, a thermally improved edge spacer has become an important element.

Window Frame

The thermal performance of the window frame has an effect on the thermal performance of the entire window. Depending on the façade type, there exist different manners of installation of the insulating glass units, such as insulating glass units with uncovered edge seals or those with mechanically retained edge seals or insulating glass units mounted in a frame which completely covers the edge seal on all four sides. The selection of the window frame often depends on the architectural design concept. However, the material of the window frame, which normally has a

higher U-value than the glazing unit, must be carefully selected. The choice can be made among wood frames, PVC frames, fiberglass frames, aluminium and steel frames with a thermal brake or composite frames made from an internal wood frame covered with external PVC or insulation-filled aluminium cladding. The U_f-value of wood frames is mainly decided by the thickness of the casement and the frame in the heat flow direction. There exist also wood frames with a number of air cavities, which additionally reduce the U_f -value. For PVC frames, the U_f -value mainly depends on the number of air cavities and the location of the load-carrying element which is usually made of metal. Window frames made of metal, usually aluminium, should be constructed of an outer and an inner profile and separated by an insulating material (a thermal break), i.e., polyamide [16]. Wood frames generally have a lower U_f-value in comparison with aluminium or plastic frames. Moreover, lower values of embodied energy make wood frames more sustainable than aluminium, PVC, steel and aluminium-cladded wood types of frames.

Other methods used for the regulation of thermal and optical performance of windows.

Apart from the parameters described above, a set of other methods can be used in order to adjust optical and thermal behaviour of windows. Contrary to the approaches already described, these methods are not static since they use either electrical voltage or chemical substances to achieve a temporary change in the light and energy transmittance. Currently, different products such as electrochromic or gasochromic windows are already either being launched or expected to reach the market in the near future. Electrochromic windows darken when voltage is added and become transparent when voltage is taken away. Such windows can be adjusted to allow for varying levels of visibility. Gasochromic windows produce a similar effect as electrochromic windows, but in order to colour the window, diluted hydrogen is introduced into the pane interspace. Upon adding oxygen, the coated surface bleaches and the window returns to its original transparent state. These contemporary products also known as *switchable glass* or *dynamic glass* represent a great potential for the use in large-size glass façades.

4.3 Research Related to the Optimal Glazing Size and Building Shape

Researching energy efficiency of buildings is not solely a matter of the last decade, as the first intensive studies related to energy and buildings date from the seventies and eighties of the previous century. Many studies focusing on the research of specific parameters that exert influence on the energy performance of buildings, such as Johnson et al. [17] and Brown [18], have been performed since then. Johnson et al. [17] systematically explored the influence of the glazing systems on the component loads and the annual energy use in office buildings typical of

different climates and orientations. Another research estimating the total area of the exposed surface of domestic buildings carried out by Steadman and Brown [18] involved an empirical study of a house plan drawn for a building in the city of Cambridge. Within a range of researched parameters, such as the relationship between the wall and the floor area, the built form, the glazing areas were examined from the viewpoint of heat loads. One of the comparable newer researches is also a parametric case study of an apartment building, fictively located in five different Turkish cities, presented by Inanici and Demirbilek [19]. The effects of variable parameters on the annual energy consumption, such as different building's aspect ratios and different south window sizes, were analysed in order to determine the optimal parameter values. Next, a parametric study of the heating and cooling demand was performed by Bülow-Hübe [20] in order to determine an optimal design for office windows in Swedish climate. Another Swedish study for 20 low-energy terraced houses built in 2001 outside Gothenburg was performed by Persson et al. [21]. The purpose of the work was to investigate how decreasing the south-oriented window size and increasing the north-oriented window size could influence the energy consumption. A number of findings are furthermore stated in the dissertation by Persson [22]; these are in certain aspects comparable to our research. In the framework of a European project Ford et al. [23], various simulations and analyses were performed for different low-energy buildings for five European countries (UK, France, Italy, Portugal, Spain) with relatively warm climates. Many of the existing studies were carried out for non-European climates. Bouden [24] investigated the appropriateness of glass curtain walls for the Tunisian local climate. The influence of windows on the energy balance of apartment buildings in Amman, Jordan, was analysed in the study performed by Hassouneh et al. [25]. In a study, focusing on the role of active systems and thermal protection in passive and plus energy residential buildings [26] explain that south-oriented windows make the solar gains outweigh the heat losses by 2/3. The relationship between the solar gains and heat losses is almost equal for south- and west-oriented windows; while for north-oriented windows, the heat losses are about 3 times higher than the solar gains.

In general, all of the presented studies deal primarily with the influence of variable parameters on the energy performance of different types of buildings (residential, offices, public) of mainly massive construction systems. From the existing research findings, we summarize that the process of defining the optimal model of a building is very complex. The most important parameters influencing the energy performance of buildings are listed below:

- Location of the building and climate data for the specific location
- Orientation of the building
- Properties of the materials installed, such as timber, glass, insulation, boards
- Building design (shape factor, length-to-width ratio, glazing size, building envelope properties, window properties)
- Selection of active technical systems.

It is therefore important to investigate the influence of the above-listed parameters with utmost care. Due to the absence of a direct correlation between the different parameters, it is more convenient to conduct separate examinations of their influence on the energy demand for buildings. The latter is of particular relevance to the influence of the building's orientation and its glazing size which will be a subject of common analysis in Sect. 4.3.1 on the one hand, and to the influence of the building shape which will be thoroughly examined in Sect. 4.3.2, on the other.

However, it is important to stress that the presented calculations do not consider various active systems' impacts (heat recovery ventilation, solar collectors, PV panels, heat pumps, etc.). The results of the comparative analysis can nevertheless serve as a good frame of reference to architects and civil engineers in an approximate estimation of the energy demands accompanying different positioning and proportion of the glazing surfaces, while using various prefabricated timber-frame wall elements.

4.3.1 Influence of the Glazing Arrangement and its Size on the Energy Balance of Buildings

One of our general critical remarks referring to the existing studies focusing on the impact of windows on the heating and cooling demand was that most of them are just calculations for a single building. In our research, an attempt at a more systematic analysis was made, with the model of a building of our base case study being performed in many variations of timber construction systems. The first part of the study presents a parametric analysis of the glazing-to-wall area ratio impact in a two-storey house with a prefabricated timber-frame structural system. The analysis was carried out for different construction systems and for different cardinal directions. Based on a parametric analysis, the second part presents a generalization of the problem related to the energy demand dependence and to the optimal glazing area size dependence on one single variable, the U_{wall}-value, which becomes the only variable parameter for all contemporary prefabricated timber construction systems, independently of their type. Finally, mathematical linear interpolation is presented as a simple method for predicting an approximate energy demand with regard to the glazing size and the U_{wall}-value in the analysed case study, thoroughly presented in Žegarac Leskovar and Premrov [27].

Among the parameters listed previously in this chapter, our case study examines the influence of the following three: the glazing-to-wall area ratio, the U_{wall}-value and the main cardinal directions for a specific climate. Since the current study limits itself solely to timber construction, which is also termed as lightweight construction, the influence of different thermal capacities of the building materials was not taken into consideration. The presented approach could be also applicable to massive construction (brick, concrete walls), if additional parameters

concerning thermal mass were considered, although we would expect slightly different results in the case of a building model in a massive construction system. Calculations do not consider various active systems impacts (heat recovery ventilation, solar collectors, PV panels, heat pumps, etc.), or various window *U*-value impacts.

4.3.1.1 Parametrical Numerical Study

The current subsection presents a parametric numerical case study of a two-storey house and its parametric analysis of the glazing-to-wall area ratio impact on the energy demand. A model was selected out of sixteen projects created in the study workshop "Timber Low-Energy House". The workshop was held upon a public call made by the Slovene timber house manufacturers. The aim of the workshop was to develop different innovative models of timber-glass low-energy houses, suitable for a typical European family of 4–5 members. Consequently, the number of occupants planned for the purposes of our parametric study was 4. The external horizontal dimensions of the model are 11.66 × 8.54 m for the ground floor and 11.66 × 9.79 m for the upper floor (Fig. 4.11). The total heated floor area is 168.40 m^2 and the total heated volume is 437.80 m^3.

The three-dimensional model of the house is presented in Fig. 4.12.

Construction

The exterior walls are constructed using a timber-frame macropanel system. All the analysed wall elements are vertical. The exterior wall U-value is 0.102 W/m^2K for the TF-3 element (c.f. Table 3.6 and Fig. 3.36c). The *U*-values of other external

Fig. 4.11 Floor plans of the base—case study model

Fig. 4.12 Three-dimensional model of the house

construction elements are 0.135 W/m^{2}K for the floor slab, 0.135 W/m^{2}K for the flat roof and 0.130 W/m^{2}K for the south-oriented overhang construction above the ground floor area. The composition of the basic TF-1 and the thermally improved TF-2 macropanel wall element is listed in Table 3.6 and presented in Fig. 3.36a, b.

Additional modifications of AGAW are made only for the south-oriented glazing areas for two classical single-panel systems TFCL-1 and TFCL-2 (Fig. 3.34a) with higher U-values. The composition of the treated single-panel timber-frame construction systems is presented in Table 4.5. The composition of the fictive single-panel wall system TFCL-3 with the U_{wall}-value of 0.30 W/m^{2}K is taken from Žegarac Leskovar [28] and Žegarac Leskovar and Premrov [27].

Glazing

A window glazing (Unitop 0.51–52 UNIGLAS) with three layers of glass, two low-emissive coatings and krypton in the cavities with a configuration of 4E-12-4-12-E4, is installed. The glazing configuration with a g-value of 52 % and $U_g = 0.51$ W/m^{2}K assures a high level of heat insulation and light transmission. The window frame U-value is $U_f = 0.73$ W/m^{2}K, with the frame width being 0.114 m. The glazing-to-wall area ratio (AGAW) of the south-oriented façade is 27.6 %, with the AGAW values of the rest of the cardinal directions being 8.9 % in the north-oriented, 10.5 % in the east-oriented and 8.5 % in the west-oriented façades.

Climate and Orientation

The house with a large glazing area installed in its longer side facing south is located in Ljubljana. The city of Ljubljana is located at an altitude of 298 m, a latitude of 46°03′ north and a longitude of 14°31′ east. According to the accessible climatic data from ARSO [29], the considered average annual external temperature is 9.8 °C. The relevant climate data are listed in Table 4.6.

Table 4.5 Composition of the analysed single-panel wall elements

TFCL-1			TFCL-2		
Material		d [mm]	Material		d [mm]
Wooden planks		22	Wooden planks		22
TSS* with open air gaps	Bitumen sheet cardboard	0.5	TSS with open air gaps	Bitumen sheet cardboard	0.5
TSS with open air gaps	Timber frame	50	TSS with open air gaps	Timber frame	20
Bitumen sheet cardboard	Timber frame	0.5	Bitumen sheet cardboard	Timber frame	0.5
MW	Timber frame	50	MW	Timber frame	80
Aluminium foil			Aluminium foil		
Particleboard		13	Particleboard		13
Gypsum plasterboard		10	Gypsum plasterboard		10
total thickness [mm]		146	Total thickness [mm]		146
U_{wall}-value [W/m^{2}K]		0.70	U_{wall}-value [W/m^{2}K]		0.48

*Timber substructure, **Mineral wool

Table 4.6 Annual climate data for Ljubljana [29]

	Annually
Average temperature	9.8
Average relative humidity at 7 am (%)	90.2
Average relative humidity at 14 pm (%)	62.4
Average duration of solar radiation (h)	1,712
Nr. of clear days (cloudiness < 2/10)	32.5
Nr. of cloudy days (cloudiness > 8/10)	142.2
Nr. of days with fog	120.8

Shading

The house is constructed with a south-oriented extended overhang above the ground floor, which blocks direct solar radiation from entering the ground floor windows during the summer, while it lets enter in winter when the angle of incidence of the sun is lower. The rest of the windows on the upper floor and those of the east- and west-oriented walls are shaded with external shading devices.

Internal Gains and HVAC

The house is equipped with a central heat recovery unit. To prevent overheating in the summer period, night ventilation with cooling through manual window is planned. The interior temperatures are designed to reach a T_{min} of 20 °C and T_{max} of 25 °C. Domestic hot water generation (DHW) and an additional requirement for space heating are covered by a heat pump with a subsoil heat exchanger and, to a minimal extent (5 %), by electric heating.

Variable Parameters

The influence on the energy demand of the following factors is studied: the glazing size in four different cardinal directions: south, north, east and west. Modifications of the glazing area size are performed in the range of AGAW from 0 % to nearly 80 % (Fig. 4.13), separately for each cardinal direction, for three timber-frame

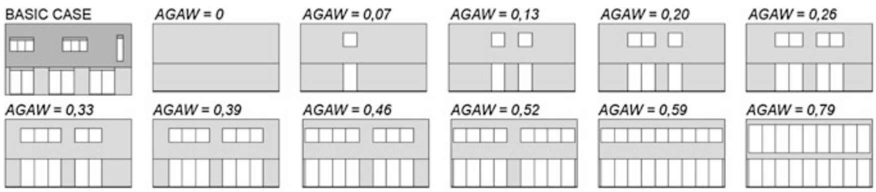

Fig. 4.13 South-oriented façade of the base—case model with the schemes of AGAW modification

macropanel systems: TF-1, TF-2 and TF-3. Modifications of the glazing area size are made step by step through adding window elements (frame + glazing) to the totally unglazed façade as presented in Fig. 4.13.

Description of the Software and the Calculation Method

The Passive House Planning Package [30] is used to perform static calculations of the energy demand. The software, certified as a planning tool for passive houses, allowing a surprisingly accurate description of thermal building characteristics of passive houses, can be also used for low-energy house design. Practice has shown that the results achieved by the PHPP software are very similar to the measured energy demand in operating buildings. It is important to stress that the main point of our study is to present an approach to optimal design. The selection of software is therefore not decisive, since many other calculation tools could be used as well. The calculation method of the parametric numerical case study process is graphically presented in Fig. 4.14. As shown, more than 160 calculations are made in order to obtain the results showing the effects of the selected parameters on the energy demand for heating and cooling. An upgrade of the calculation procedures

Fig. 4.14 Scheme presenting the calculation method

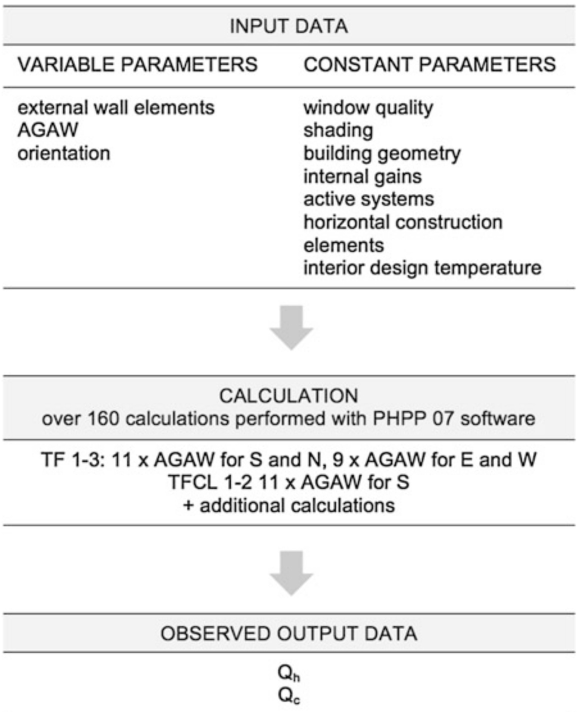

will be presented later in this paper with the generalization of the results for one single-variable parameter (U_{wall}-value).

4.3.1.2 Results and Discussion

Figure 4.15 shows a comparison of the annual energy demand for heating (Q_h) as a function of the glazing area size for different cardinal directions of the TF-3 construction system with the lowest U_{wall}-value.

The results show evidence of the strongest influence of increasing the glazing area size in the south orientation where Q_h decreases almost linearly with a growing AGAW and the heat gains at AGAW = 0.79 add up to almost 52 % of the Q_h value at AGAW = 0. The increase in Q_h for almost 37 % related to the energy demand for heating at the starting point shows that the influence of altering the glazing area size facing north is less expressive than that of its southern counterpart. The east and west orientations, on the other hand, show almost identical behaviour.

The presented analyses generally accord well with the results of the parametric study research on the effect of the glazing type and size on the annual heating and cooling demand for the Swedish timber-frame offices [20] and low-energy houses [21, 22]. Taking into account the differences in climate, there is considerable agreement noticed with certain statements from design guidelines for comfortable low-energy homes considering the climate in Milan [23]. Furthermore, the obtained results show a relatively good coincidence with the values for the energy demand related to different glazing area sizes with different glazing types for the case study in Amman [25], with respect to certain differences in the external air temperature and the duration of solar radiation considered in the calculations.

The behaviour of the energy demand patterns of the TF-1, TF-2 and TF-3 systems for the west and east directions is very similar, while the patterns for the north orientation show only the increase in the energy demand. No noticeable decrease in the energy demand, either for Q_h or Q_c, appears for the north, west or east orientations. Therefore, only the south direction, the focal point of our special interest, is additionally analysed and compared for all construction systems. The most interesting point is the comparison of the sum total of the energy demand

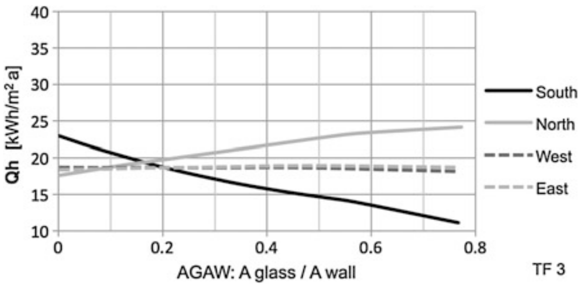

Fig. 4.15 Annual energy demand for a heating (Q_h) in the TF-3 construction system as a function of AGAW for different cardinal directions

$(Q_h + Q_c)$ for different construction systems (TF-1 to TF-3), presented in Fig. 4.16. In the case of timber buildings, particular attention should be paid not only to the energy demand for heating, but to that for cooling as well. Due to a low thermal capacity of timber, the risk of overheating is considerably higher than in buildings made of brick or concrete.

The results for the sum total of the energy demand show an interesting phenomenon related to the optimal point with the lowest $Q_h + Q_c$ demand which is clearly evident in the TF-3 construction system, appearing at the range of AGAW ≈ 0.34–0.38, quite evident in the TF-2 system at AGAW ≈ 0.41 and less evident in the TF-1 system at AGAW ≈ 0.42–0.50. We assume that the optimal share of the glazing surface in the south-oriented exterior walls depends on the thermal transmittance of the exterior wall. The optimal share of the glazing area in walls with extremely low U-values is smaller than in walls with higher U-values. If we pay attention to the behaviour of the $Q_h + Q_c$ function curve after reaching the optimal point, we notice that the sum total of the energy demand for heating and cooling increases more in the TF-3 construction system, which has the lowest thermal transmittance, while in the TF-1 system with a higher U_{wall}-value, the function converges. The higher the U_{wall}-value of a specific system, the higher the values of the functional optimum.

It is interesting to compare the results with the study performed by Inanici and Demirbilek [19], who showed that in the process of increasing the south-facing window area, each increase in the glazing size led to a decrease of the total energy load $(Q_h + Q_c)$ for cool climates, while the opposite was true of hot climates. Due to a method of keeping a constant overall U_{wall}-value, a direct comparison with our case is not possible, although the analysis for Ankara, whose average annual temperature is similar to that of Ljubljana, showed interesting results when an additional calculation method was used. The lowest energy loads were shown at the maximal U_{wall}-value and the glazing-to-wall area ratio of 30 %, which is similar to our case.

For comparison purposes as well as for support in setting up the basic principle of the glazing surface impact on the energy behaviour patterns, an analysis of the classic single-panel prefabricated wall elements is carried out, but only for the south orientation. Firstly, TFCL-2 and an additional fictive wall element TFCL-1

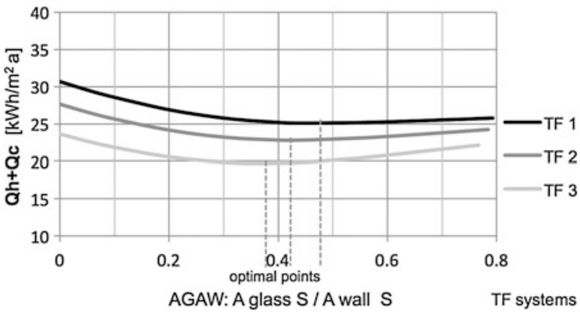

Fig. 4.16 Comparison of the sum total of the energy demand for heating and cooling as a function of AGAW for the south orientation of the selected TF construction systems (TF-1 to TF-3)

Fig. 4.17 Comparison of the energy demand for heating and cooling as a function of AGAW for the south orientation of the selected TF construction systems

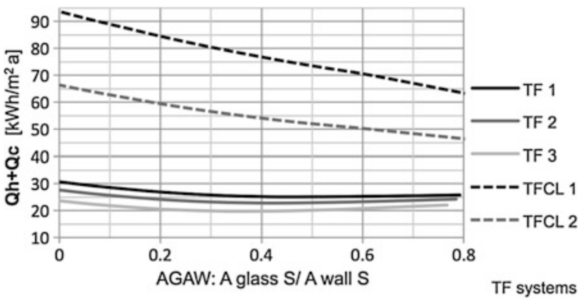

are analysed. Thermal properties of the selected wall elements do not satisfy even the basic requirements for the thermal transmittance of an exterior wall (U_{wall}-value < 0.20 W/m^{2}K for a lightweight construction) in low-energy house design. The analyses of the sum total of the heating and cooling demand presented in Fig. 4.17 seem to be most interesting.

It is evident from the presented results that at higher U_{wall}-values of the exterior wall elements, the functional optimum (the lowest $Q_h + Q_c$ value) disappears, the $Q_h + Q_c$ function curve passes from parabolic dependence in construction systems with extremely low U_{wall}-values (TF-2 and TF-3) to linear dependence in construction systems with high U_{wall}-values (TFCL-1 and TFCL-2). The inclination of the function line presenting TFCL systems depends on the U_{wall}-value. Energy decrease caused by an increase in the total glazing area (measured from AGAW = 0 to AGAW ≈ 0.80) represents approximately 33 % of the starting point value for the TFCL-1 system, but only 17 % for the TF-3 system with the highest insulation features (measured from AGAW = 0 to AGAW$_{\mathrm{opt}}$).

4.3.1.3 Generalization of the Problem to One Single Independent Variable (U_{wall}-value)

Determination of AGAW$_{\mathrm{opt}}$

The main aim of the presented study is in developing a theoretical approach applicable to architectural design of an optimal energy-efficient prefabricated timber-frame house. It is thus important to transform this complex energy-related problem, dependent on the structural system, to only one single independent variable (U_{wall}-value) which becomes the only variable parameter to determine the optimal glazing area size value (AGAW$_{\mathrm{opt}}$) for all contemporary prefabricated timber construction systems.

The first step to be taken in setting up the basic theory of the research focusing on a single independent variable is to observe and compare the energy demand behaviour for both, the new macropanel wall elements and the classic wall elements with single-panel construction, where the thermal transmittance of the selected wall elements is fictively set at an equal value. In Fig. 4.18, we present the comparison of

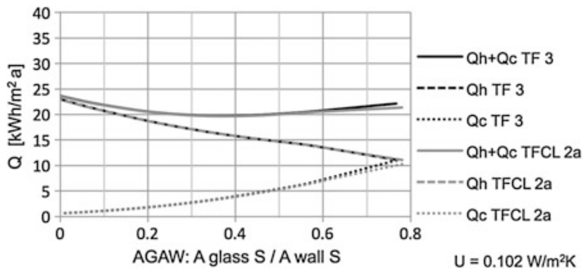

Fig. 4.18 Comparison of the energy demand as a function of AGAW for the south orientation of the selected TF-3 and TFCL-2a construction systems with a uniform U_{wall}-value = 0.102 W/m^{2}K

the sum total of the energy demand ($Q_h + Q_c$) for TF-3 and TFCL-2a construction systems, where the wall elements with an equal U_{wall}-*value* = 0.102 W/m^{2}K are analysed. The U_{wall}-value for TFCL-2a system is obtained by adding fictive insulation to the single-panel TFCL-2 wall element.

For the benefit of further approach, it is important to notice that the results presented in this particular case are almost equal for both construction systems. Additionally, we also analysed three different massive panel CLT systems (types KLH-1, KLH-2 and KLH-3) described in Sect. 3.2.2.2 and schematically presented in Fig. 3.22. The whole analysis with the calculated results is presented in Žegarac Leskovar [28]. The calculated results for the optimal AGAW values of all the analysed types of external wall elements are seen in Table 4.7.

Based on the results presented, it is now possible to analyse the relationship between the optimal glazing size in the south-oriented external wall elements (AGAW_{opt}) related to the $Q_h + Q_c$ energy demand and the thermal transmittance of the wall element (U_{wall}-value). The data presented in Fig. 4.19 show the values of AGAW, at which the $Q_h + Q_c$ demand reaches the lowest value, depending on the U-value of the external wall element as the only independent variable.

Figure 4.19 shows that the optimum or the convergence of the function curves for AGAW_{opt} appears only in systems with a U_{wall}-*value* $\leq$ 0.193 W/m^{2}K. As the U_{wall}-value increases, the optimal share of south-oriented glazing size becomes higher. Upon reaching the limiting U_{wall}-*value* = 0.193 W/m^{2}K, the values of the optimal AGAW converge towards the maximal glazing surface. No optimum or convergence for AGAW appears in the analysed construction systems with an

Table 4.7 Optimal values of AGAW in south-oriented external wall element for selected timber construction systems

Construction system	U_{wall} [W/m^{2}K]	AGAW_{opt}	AGAW_{opt} adjusted
TF-1	0.164	0.42–0.50	0.47
TF-2	0.137	0.41	0.41
TF-3	0.102	0.34–0.38	0.37
KLH-1	0.181	0.52–0.54	0.53
KLH-2	0.148	0.41–0.46	0.43
KLH-3	0.124	0.38–0.40	0.39
Systems	$\geq$0.193	$\approx$0.80	0.80

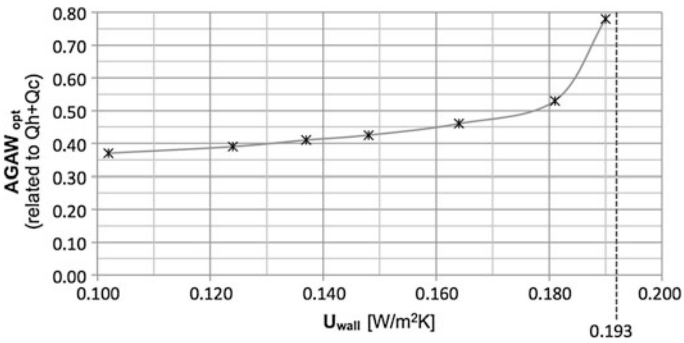

Fig. 4.19 Optimal values of AGAW in the south-oriented external wall element as a function of the U_{wall}-value for timber construction systems

U_{wall}-value > 0.193 W/m^{2}K. Although the lowest $Q_h + Q_c$ is reached at the maximal AGAW value, we have to pay attention to the data for the overheating frequency.

In conclusion, it is important to stress that the existing literature offers only predictive and in many cases even clearness-lacking parametric studies on the optimal glazing size depending on thermal characteristics of the external wall. Due to a large list of parameters affecting the energy performance of a building, it is important to assure a way to a fast and simple pre-estimation of the energy load. In contrast, the scientific contribution of the current study is presented by analytical functional dependence of AGAW on the U_{wall}-value (Fig. 4.19), which allows for a selection of any external wall element with a specific U_{wall}-value and consequently for a selection of an optimal AGAW value, which increases with the increase in the U_{wall}-value.

The presented generalization concerning the U_{wall}-value as the only variable parameter can be applied to timber construction in general, regardless of the construction system. The determined function for the optimal south-oriented glazing size (AGAW$_{\text{opt}}$) offers an opportunity to select an optimal renovation process that would combine the improvement of thermal properties of the external walls through an additional layer of insulation, with the installation of the optimal glazing size which is noticeably smaller in the case of a lower U_{wall}-value.

4.3.1.4 Use of the Linear Interpolation for a Simple Pre-estimation of the Energy Demand

In order to set the next general principle, a graphical presentation (Fig. 4.20) of the sum total of the energy demand for heating and cooling as a function of the U_{wall}-value for the three selected AGAW values (AGAW $= 0$, AGAW ≈ 0.40, AGAW ≈ 0.80) is of great importance. The results of the parametric numerical case study (Fig. 4.20) feature the $Q_h + Q_c$ demand for three glazing-to-wall ratios,

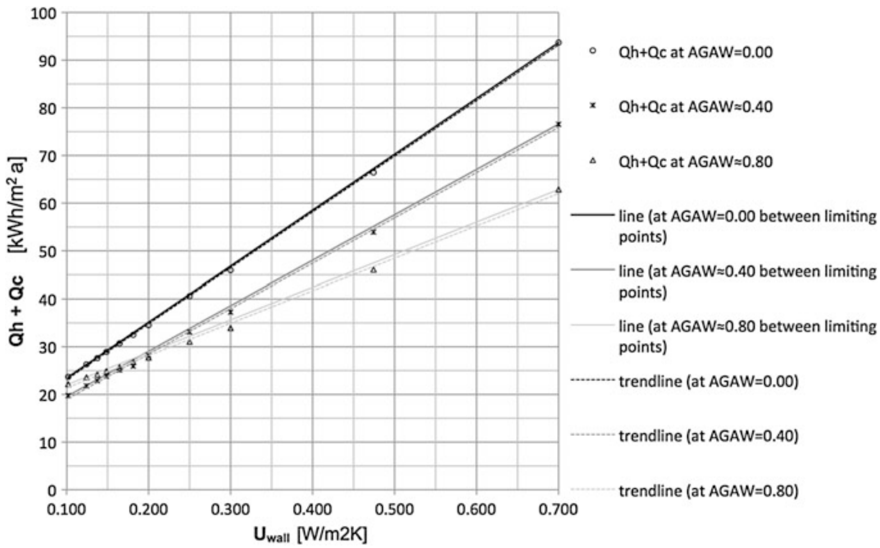

Fig. 4.20 $Q_h + Q_c$ demand as a function of the U_{wall}-value for three different AGAW values with possible ways of linearization

for AGAW = 0, AGAW ≈ 0.40 and for AGAW ≈ 0.80, along with possible ways of linearization.

The $Q_h + Q_c$ demand increases almost linearly with the increase in the U_{wall}-value. The values for the sum total of the energy demand for all three AGAW values are almost straight lines with an inclination angle depending on the AGAW value. Another item of importance is seen in the fact that the linear approximation between the two limiting selected points of the U_{wall} produces nearly the same results as the straight line with the smallest deviation. The process of calculation can thus become substantially shorter and simplified.

The linearization of the energy loads ($Q_h + Q_c$) problem shows that the use of linear interpolation is very simple and applicable, owing to the fact that it includes the influence of both important functional variables, the U_{wall}-value and AGAW. In that manner, it can be used by architects to obtain a very fast and simple estimation of the expected energy loads when designing a building with a precisely defined thermal transmittance value of the exterior wall elements (U_{wall}-value) and a selected share of the glazing area in the south-oriented façade (AGAW).

4.3.2 *Influence of the Building Shape*

Designing timber-frame houses with enlarged glazing surfaces offers numerous possibilities of creating structures with a highly attractive shape. Nevertheless,

some of the existent studies prove that an attractive and dynamic building design usually results in increased energy demand. The main aim of the current study therefore is to present design solutions where the above increase could be avoided by selecting the appropriate size of the glazing surface in the south façade. Al Anzi et al. [31] investigated the impact of relative compactness (RC) on the annual cooling energy use and the annual total building energy in Kuwait. Their research was based on a prototypical building with over 20 floors and the relevant simulation analysis incorporated several building models with various shapes (L, U, T, cut shape, cross-shape, trapezoid). The impact of the window to wall ratio and that of orientation on the energy use were analysed with respect to various window sizes and glazing types. Furthermore, [32] studied the relationship between the shape and energy requirements during the winter season in two French localities with different climate conditions. They found no correlation between the energy consumption of a building and its shape in a mild climate. Another interesting research is the parametric study by Inanici and Demirbilek [19], whose results show no major influence of the length-to-width ratio on the energy performance of a building when specific climatic conditions are taken into account.

In professional practice, the most used index to describe the shape of the building is the *shape coefficient* (F_s) defined as the ratio between the envelope surface of the building (A) and the inner volume of the heated volume of the building (V) given in the form of Eq. (2.2). Albatici and Passerini [33] were encouraged to research new indicators of the energy performance within mild and warm climate conditions related to the building shape. They presented heating requirements of buildings with different shapes in the Italian territory. Their research based on a monthly method (simplified approach) confirms that compactness is more important in cold localities. Hence, the introduction of a new simplified index, the *south exposure coefficient* (C_{fs}):

$$C_{fs} = \frac{S_{south}}{V} \tag{4.2}$$

where S_{south} represents the surface of the south-oriented façade. Having taken heating requirements into account, Albatici varied envelope areas of the models, while the volume and the percentage of the glazing remained constant.

Another important parameter often used to determine solar access of a building, assuming that the latter is of a given height and optimally oriented, is the aspect ratio (AR), a ratio between the building's length and width (AR = L/W), already presented in Sect. 2.5.1. All the parameters are schematically presented in Fig. 2.8. The aspect ratio is a significant parameter in energy-efficient design concerning the building shape, as emphasized in several studies. In cold climates, for example, the ideal aspect ratio for a rectangle-shaped solar house design ranges from 1.3 to 1.5 [34]. Hachem et al. [35] investigated the effects of the geometric shapes of two-storey single-family housing units on their solar potential by using the so-called *depth ratio a/b*, where a represents the length of the shading façade and b the length of the shaded façade (Fig. 2.9). The paper demonstrates that both

parameters control the extent of shading and consequently a reduction in the solar radiation incident on the shaded facade. It is therefore desirable to reduce the depth ratio in order to optimize the solar potential of façades. A rectangle, with the aspect ratio of 1.3, serves as the reference.

The main aim of the numerical study to be presented is to establish the optimal building shape factor (F_s) with the optimal size of the south-oriented glazing surface for residential timber buildings from the point of view of the energy performance. Two different locations with different macroclimate conditions and solar potential are analysed. The study, solely limited to timber construction, analyses the exterior wall elements in passive design, assuming that the rest of the parameters, such as active technical systems, roof and floor slab assemblies, remain constant. Many of the findings can be beneficial to architects in designing new timber buildings or renovating the existing ones and serve as systematic guidelines for a quick estimation of the building's energy performance, even in the case of highly attractive timber-glass building shapes.

4.3.2.1 Parametric Study: Simulation Model

The presented numerical research is based on a case study of a 3-metre-high one-storey house built in the prefabricated passive timber-frame structural system. The ground floor area ($A_f = 81$ m^2), the heated volume ($V = 243$ m^3) and the percentage of the glazing size in the south façade (AGAW) are kept constant. The calculations are done for the value of $\mathrm{AGAW_{opt}} = 0.35$, which is the optimal size of the glazing placed in the south façade with the external wall standard of $U_{\mathrm{wall}} = 0.10$ W/m^{2}K. A window glazing (Unitop 0.51–52 UNIGLAS) with three layers of glass, two low-emissive coatings and krypton in the cavities for a normal configuration of 4E-12-4-12-E4 is installed. The glazing configuration with a g-value of 52 % and $U_g = 0.51$ W/m^{2}K assures a high level of heat insulation and light transmission [16]. The window frame U-value is $U_f = 0.73$ W/m^{2}K.

On the other hand, the building design and consequently its shape factor ($F_s = A/V$) vary parametrically. Variations of square, rectangular, L and U shapes of the building were analysed with a total of 8 different ground floor shapes (Fig. 4.21). The building shape factor (F_s) varies parametrically from 1.47 to 1.76.

Climate data for two cities located in different climate conditions, Ljubljana and München, were taken into consideration with a view to getting feedback on the influence of the building shape exposed to different solar radiation. The computer-based analysis Ecotect [36] was used to perform the calculations.

4.3.2.2 Parametric Study: Results and Discussion

The calculated numerical results for the transmission losses (Q_t) through the external walls and the solar gains (Q_s) through the glazing placed in the south façade are presented for both locations, München and Ljubljana (Fig. 4.22).

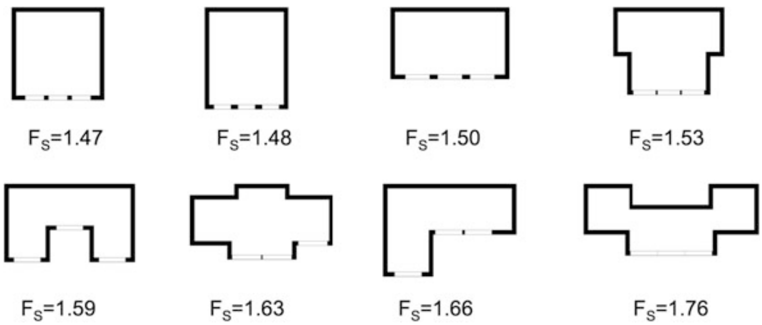

Fig. 4.21 Considered variations of the ground floor shape of the building

The difference between the transmissions heat losses and the solar heat gains increase almost linearly with the shape factor. The reason lies in the fact that the size of the building envelope increases with the dynamics of the building shape. It is, however, important to stress that the function inclination for München is evidently higher than that for Ljubljana.

In order to make further conclusions about the influence of the building shape factor on the annual energy demand of a building, it is important to take into consideration the entire heating and cooling periods. Figures 4.23 and 4.24 therefore show the results for the annual heating and cooling demand for Ljubljana and München. The annual heating demand was calculated by Eq. (2.1) and schematically presented in Fig. 2.2.

Both diagrams point to an interesting dissimilarity between the total annual energy demands for the compared cities, observed at an increased building shape factor. Owing to a lower inclination of the function line presenting the $Q_t - Q_s$ values for Ljubljana (Fig. 4.22) and due to the influence of an increased shape factor value on the cooling demand, the total annual energy demand for the

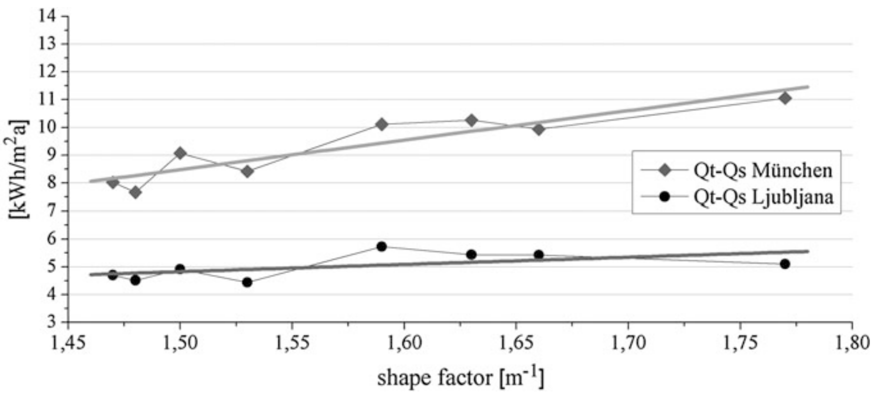

Fig. 4.22 $Q_t - Q_s$ diagrams in dependence on the shape factor for München and Ljubljana

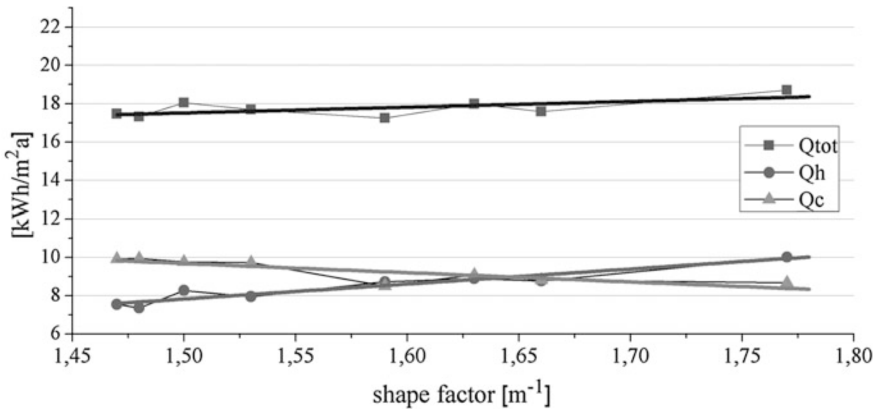

Fig. 4.23 Energy demand for heating (Q_h), cooling (Q_c) and the total energy demand (Q_{tot}) for Ljubljana

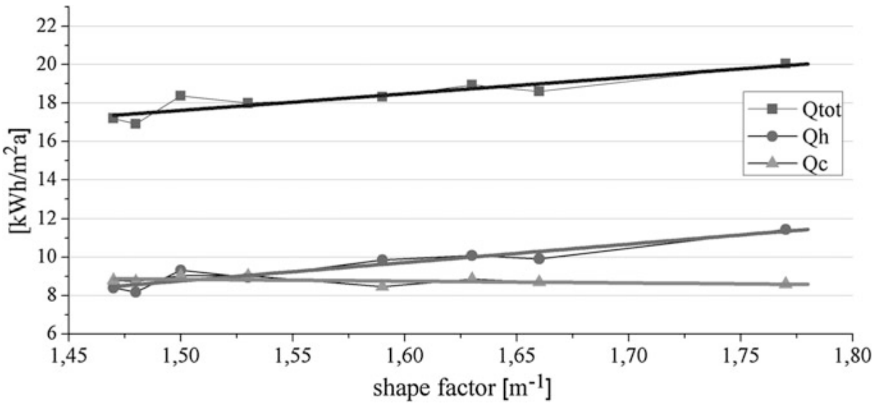

Fig. 4.24 Energy demand for heating (Q_h), cooling (Q_c) and the total energy demand (Q_{tot}) for München

building in Ljubljana is almost independent of the building shape factor. The latter finding is rather contradictory to some well-known existing studies claiming that attractive and dynamic building design usually results in the energy demand increase. The results for the building located in München, on the other hand, are less encouraging (Fig. 4.24) with the influence of the building shape on the total energy demand being far more significant, on account of higher transmission and lower solar radiation in the winter period.

The performed parametric analysis evidently proves that modern passive prefabricated timber-frame buildings with the optimal size of the triple glazing placed in the south façade allow for designs incorporating a more complex ground plan and a more attractive design, which results in increasing the value of the building

shape factor. This finding is in contradiction to most of the existing studies performed on different buildings shapes. The building in Ljubljana demonstrates an almost constant value of the total energy demand for heating and cooling at an increasing value of the building shape factor, which is due to the fact that the solar heat gains through the glazing placed in the south façade increased in an almost similar way as the transmission losses. Nevertheless, the results show a less encouraging outcome for the locations with lower solar radiation, as compared to our study case of München. Our conclusion resembles some of the findings by Albatici and Passerini [33], given for the Italian territory.

4.4 Structural Stability of Timber-Glass Houses

Modern houses design focuses on ensuring high indoor comfort quality and low-energy consumption. Investors and architects decide upon the orientation of a building and its transparent areas with a view to maximizing the use of natural solar radiation gains. The latter is preconditioned by the appropriate size and orientation of large transparent areas which have to transmit an adequate amount of solar energy into a building in order to provide for natural lighting and heating of the interior space. A comparison of transmission losses through the building envelope with the possible solar heat gains in order to achieve the optimal energy demand of the house is of a great importance in defining the optimal size of glazing areas and a suitable selection of the glazing type.

With respect to the above facts, discussed and analysed in Sect. 4.3, a major part of the glazing needs to be installed in the south-oriented façade for the purpose of better energy performance of a building, which leads to specific technical challenges in the field of structural behaviour of the load-bearing wall elements with an enlarged glazing size. Even though energy-efficient, such construction systems can be extremely problematic when the building is exposed to horizontal loads.

Two of the typical horizontal load cases are wind and earthquake. Their load distribution through the building is the same (Figs. 3.39 and 3.40) although the effects on the building and the subsequent consequences prove to be different. The earthquake, which implies a rapid high intensity dynamic load on the building leading to catastrophic outcomes, is definitely a more concern causing horizontal load case.

One of the basic principles incorporated in designing a building to withstand seismic loads is avoiding *plan irregularity*, i.e., providing for a uniform lateral stiffness distribution in a building. Hence, we eliminate the risk of unfavourable torsion effects which occur with dynamic loads acting upon an irregular floor plan and increase the seismic load on the structure. Energy-efficient buildings with enlarged glazing areas predominantly placed on southern façades may therefore make proper seismic design of the building become a rather difficult and problematic task.

In addition, transparent glass areas usually provide hardly any horizontal stiffness and cause substantial decrease in structural stability of a single-wall assembly. Method A in Eurocode 5 [59] defines that wall panels containing a door or window opening should not be considered as contributing to the racking load-carrying capacity. Method B is less restrictive and declares that the lengths of the panel on each side of the opening formed in the panel should be considered as separate panels. Nevertheless, the use of the most accurate numerical FEM approach (Sect. 3.3.1) reveals that wall panels containing a door or window opening decrease the racking resistance and significantly lower the horizontal stiffness of prefabricated frame-panel wall elements on the one hand, but can still contribute to the horizontal stability of the entire wall assembly on the other. The decreasing factor for the horizontal resistance and stiffness depends on the size and position of the openings.

Section 3.4 discussed a problematic area relating to the horizontal stability of multi-storey timber-frame buildings and presented various options of strengthening prefabricated wall elements in lower storeys where the horizontal load impact is the highest (Fig. 3.52). The horizontal load at the top of the wall element is shifted over the connecting plane and the sheathing board to the support (Fig. 3.46). The sheathing board thus assures the horizontal stability of the entire element.

The main idea of using fixed glazing in prefabricated timber-frame-panel wall elements is to replace the classical sheathing boards with glass panes, as seen in Fig. 4.25.

Contribution of glass areas to the stiffness has been so far rather neglected, which can be accounted for by a relatively low strength and ductility levels of ordinary glass used for windows. However, the introduction of modern glass materials, such as tempered and laminated glass or glass-fibre-reinforced polymers

Fig. 4.25 Timber-glass prefabricated walls—replacing the classical sheathing boards with the glass panes

(GFRP) along with the improvements of glass products' strength properties has allowed for the use of large glazing surfaces since they now contribute to the horizontal stiffness and resistance of the wall elements. The function of sheathing boards is thus taken by glass panes whose stiffness assures the horizontal stability of the wall element. The horizontal point load acting at the top of the element is consequently transferred to the supports in the same manner as already presented in Fig. 3.46:

- The adhesive takes over the shear stresses in the gluing line.
- The tensile diagonal of the glass pane shifts the force to the support.

Application of glass panes acting as load-bearing structural elements in the in-plane stress distribution assures the horizontal stability of the building and replaces the usage of visible diagonal elements (Fig. 4.26). Stability problems which can appear in the case of lower-storey wall elements with large glazing areas are solved by the use of steel diagonals. The latter is a common engineering practice to assure stability of the building against horizontal load actions (Fig. 4.26). Inserting diagonal steel elements is often seen as a less desirable option as it tends to cause heat bridges and turns the erection of the building into a complicated manoeuvre. A timber frame with steel connections is another solution, although not an ideal one since it requires large quantities of steel and provides little stiffness in comparison with full wall segments.

One of the main disadvantages of glass as a load-bearing material is its brittleness. Appropriate seismic design relies on the ductility of materials in order to dissipate the earthquake energy and avoid brittle mechanism failures. Notwithstanding the above, although brittle, modern glass proves to be a very strong material with high compression and tension strengths. If properly connected to the framing system via ductile connectors, it could form a potential lateral stiffness system with the capacity of withstanding earthquakes.

Combining timber and glass to make an appropriate load-bearing element is a very complex process involving a combination of two materials with different

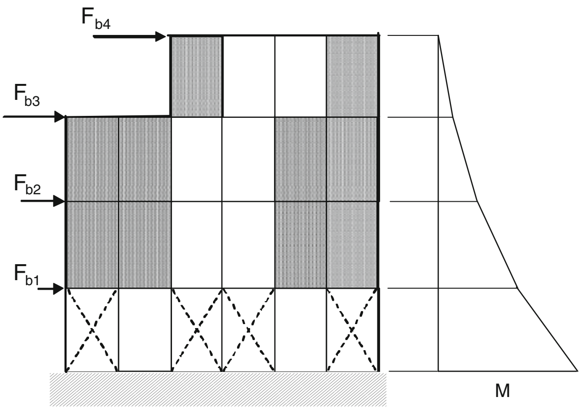

Fig. 4.26 Horizontal load distribution in a multi-storey timber-glass building

material characteristics, described in Sects. 3.1 and 4.1. The external timber-glass wall elements will be mostly placed in the southern façade of the building and thus exposed to extreme temperature changes, in view of which it is important to stress the different coefficients of thermal linear expansion (α_t) of glass and timber in the grain direction (with the coefficient of glass being two times higher than that of timber). The coefficient of thermal expansion for timber perpendicular to the grain is as much as ten times higher than the coefficient for timber parallel to the grain direction [37] and therefore almost twenty times lower than that of glass. Consequently, an increased temperature effect may increase the shear stress appearing in the adhesives between both materials. Furthermore, design of timber-glass wall elements functioning as load-bearing elements against seismic loads needs to focus on assuring the static resistance of the building in addition to that of its high ductility. Another vital matter to be discussed is an almost complete absence of the remaining load capacity after the appearance of the first crack in the glass panes, which opens a question of finding adequate balance between strength and flexibility of such composed elements. Hence, there is a need for the development of a ductile connection system between timber and glass, a system which can assure high static resistance and take over static loads only (dead load, live load, snow, etc.). According to the presented facts, we can conclude that there is a certain "game played" by the strength and ductility, while the boundary conditions between timber and glass can be classified as having the most important role in the design of such composed elements.

There are also other parameters which can exert significant influence on the horizontal resistance and stiffness of the timber-glass wall elements, such as material characteristics and the thickness of glass panes, even though the boundary conditions between timber and glass tend to be classified as the most important. The above boundary conditions in wall elements are subject to the following most influential parameters:

- Position of the glass pane and consequently the position of the glue line
- Type of the adhesive
- Thickness and width of the glue line.

The three parameters have already been studied by several authors, experimentally and numerically, and will therefore be only briefly presented.

4.4.1 Experimental Studies on Wall Elements

Glass panes were more often used in steel frame systems than in timber-frame systems to assure horizontal stability of the buildings, which calls for a brief overview of some important findings from studies performed on steel frame elements. The emphasis of our discussion will be laid on the conclusions which can be adopted also for the timber-frame wall elements. In the buckling test on the square panes with a four-sided support exposed to a continuous linear compression

in-plane load, [38] proves that the ultimate flexure tensile strength of glass depends on the duration of the exposure to load, on surface damage of both panes and on the level of the residual stress during the tempering process. Since the panes are made of heat-strengthened laminated glass, the main parameter for the buckling capacity of the laminated glass is shear stiffness of the PVB interlayer foil, with the remaining two parameters being the thickness of glass and initial surface imperfections.

A possibility of replacing compression elements with glass panes acting as elements of stabilization in modern shell structures was presented by Wellershoff [39]. Using analytical models and an experiment, two different structural systems were developed. System A represented a hinged metal frame with a lever and discrete joints in the frame nodes while system B represented a glass pane which was adhesive bonded to both sides of the metal frame and functions as the shear wall. The adhesives applied were acrylates and polyurethanes, with glass being laminated and heat-strengthened. The two systems were subjected only to in-plane loads or to the combination of the in-plane and out-of-plane loads. System B activated tensile diagonals, in addition to revealing three areas of the highest tension, i.e., in the middle of the glass pane along the tensile diagonal, at the corners of the glass pane—at the starting and the end points of the compression diagonal and finally, at the anchoring point of the adhesive bonded joint. His experimental researches additionally focused on the influence exerted by the duration of exposure to load and by environmental situations, such as UV radiation, humidity and temperature. The adhesives applied were silicones, acrylates, polyurethanes and epoxy. Wellershoff came to a conclusion that the shear stiffness of polyurethanes and acrylates was higher than that of silicone. On the other hand, with the increase in temperature, the shear stiffness of polyurethanes and acrylates was decreased while the stiffness of the silicone remained unaltered. Weller [40] tested the same adhesives as Wellershoff. Adhesive bonding of glass for construction purposes is feasible in practice under the condition of acquiring consensus permits for structures and joints of this kind, ascertains the author.

Adhesive bonding of insulating glass to be installed in winter gardens, façades, residential buildings, etc., was studied by Schober et al. [41]. The test specimens measuring 1.25×2.5 m represented a double insulating glass plate linearly adhesive bonded to the timber frame using acrylates and silicone adhesives. An interesting example of testing glass panes in the steel frame subjected to in-plane and out-of-plane loads can be seen in the research by Močibob [4]. Two concepts of lateral and vertical in-plane load shifts along with a continuous linear out-of-plane load shift were studied. The first was a point support concept with the second being a linear support concept. Both concepts successfully underwent testing as well as exposure to in-plane and out-of-plane loads. The glass used was heat-strengthened and laminated, bonded with construction silicone. According to the author's findings, the lateral in-plane stiffness increases proportionally to the higher thickness of glass and the pane fails in the compression diagonal since the tensile diagonal can no longer support the compression diagonal. Furthermore, Močibob asserts that in-plane and out-of-plane displacements prior to failure are

rather high. Peripheral bonding of glass panes onto a metal frame was studied also by Huveners [42] who produced experimental, analytical and numerical proof of the possibility of using such bracing elements in glass façades and single-storey buildings. The test specimens were made of square-shaped toughened glass with a thickness of 12 mm and the size of 1.0 × 1.0 m. Having developed three different models according to the type of adhesive, the author finds out that epoxy adhesives prove to be more suitable than polyurethanes as their use helps to attain higher in-plane stiffness.

One of the first instances of using glass panes as load-bearing elements in combination with *lightweight timber structures* was presented by Niedermaier [43], according to whom glued joints can be normally classified into three different types (Fig. 4.27). Joint type 1 is a polyurethane or silicone end joint, joint type 2 is a two-sided epoxy joint and joint type 3 is a one-sided epoxy joint. Generally, joint type 2 demonstrates larger stiffness than joint types 3 and 1.

Niedermaier experimentally studied the shear strength of glass panel elements in combination with timber-frame constructions. He tested stiffening glass panel elements which were 800 mm wide and 1,600 mm high. The glass pane was fixed to the timber frame using a joint type 3 with the glue line dimensions of 12-mm-wide and 6-mm-thick polyurethane or silicone adhesive. A horizontal load of 1 kN was applied on the top member. The research results show that the deformability of the timber frame and the tension distribution in the glass depend on the geometry of the adhesive bonded joints as well as on the type of adhesive.

A number of studies on combining glass with timber and those on the in-plane load-bearing capacity of glass panes in *timber-frame wall elements* have been so far carried out by Holzforschung Austria [44] and the Technical University of Vienna [45, 46], which will be of assistance in the comparison with our experimental results. The glazing placed on the external side of the timber frame was not directly glued to the timber frame but bonded with adhesives to the special substructure (Fig. 4.28) which is fixed with bolts to the external side of the timber frame. The entire system was protected by the patent HFA Pat.-Nr. 502470. The most important technological advantage of such type of connection is a relatively simple replacement of the glazing replacement in the case of its breakage.

Fig. 4.27 Adhesive joint types presented by Niedermaier [43]

Fig. 4.28 Connection of the glazing to the substructure and the timber frame in HGV elements, adopted from Neubauer and Schober [44], Holzforschung Austria, Pat.-Nr. 502470

In the experimental analysis, Silicone A with the shear modulus $G = 0.37$ MPa and the glue line dimensions of 14 and 19 mm/3 mm in addition to acrylate with the shear modulus $G = 2.0$ MPa and the glue line dimensions of 14 mm/2 mm were used. A single float-glass pane with a thickness of 8 mm and outer dimensions of 1,250 × 2,500 mm was used to assure the horizontal resistance of the tested elements. Timber-frame elements with dimensions of the cross section of 60/160 mm were composed of timber class GL 24 h. The elements were tested with the horizontal point load acting at the top of the wall and supported by two supports, the tensile and the compressive (Fig. 4.29). The cyclic load procedure (0.1–0.4–1.0 F) according to [47] was performed.

The results for all types of adhesives are presented in Table 4.8. The results measured in the test samples with classical OSB 3 sheathing boards are given for comparison purposes only.

Fig. 4.29 The HGV test samples were subjected to the horizontal point load at the top edge [45]

Table 4.8 Experimental results [44, 45]

Type of the adhesive	Dimensions of the glass panes [mm/mm]	Number of the test samples	Dimensions of the glue line [mm/mm]	Failure force F_u [kN]	Force at $u = h/500$ F_h [kN]	Horizontal stiffness K_h [N/mm]	Slip in the glue line [mm/kN]
Silicone A	1 × 1,250/2,500	$n = 5$	14/3	13.39	2.98	594	0.22
Silicone A	2 × 1,250/2,500	$n = 2$	14/3	24.74	6.76	1,347	0.09
Silicone A	1 × 1,250/2,500	$n = 3$	19/3	21.95	5.12	1,022	0.12
Acrylate	1 × 1,250/2,500	$n = 6$	14/2	38.68	0.62	2,885	0.006
OSB 3	1 × 1,250/2,500		/	34.50	1.30	1,358	/

Although the Silicone A test samples with the 14-mm-wide glue line demonstrated the average failure force at $F_u = 13.39$ kN, it is important to stress that the force occurring at the horizontal displacement of $u = h/500 = 5$ mm was only $F = 2.98$ kN. We can therefore conclude that the horizontal stiffness of the test samples was extremely low. The failure force of the test samples rapidly increased with the width of the glue line. The test samples with a 19-mm-wide glue line demonstrated the average failure force at $F_u = 21.95$ kN, which meant an increase of 64 %. The value of the force at serviceability limit state condition demonstrated a more rapid increase towards the value of $F_h = 5.12$ kN and a subsequent increase in stiffness by 72 %.

It is furthermore interesting to compare the results of the test samples with a single glass pane with those having two glass panes, both placed on the external sides of the timber-frame elements. The results demonstrate an increase in the failure force of 85 % and an increase in the stiffness of 127 %. This finding can be of assistance in designing timber-frame-panel multi-storey buildings located in heavy windy or seismic areas.

As described at the beginning of the chapter, a general construction-related goal is to replace the classic sheathing boards (wood-based or fibre-plaster boards) with glass panes. A comparison of the measured results obtained for the wall elements with glass panes with those relevant to the elements with the classical OSB boards witnessed a considerable reduction in the load-bearing capacity and stiffness. The failure force of the test samples where the Silicon A adhesive with a 14-mm-wide glue line was applied exhibited merely 39 % of the failure force of the element with the OSB boards. The stiffness underwent a similar, 44 % reduction.

Appropriate resistance of the wall elements with glass panes demands application of acrylate adhesives which make the slip in the glue line evidently smaller than silicone adhesives. The load-bearing capacity and the stiffness in particular were noticeably higher than in elements with OSB boards. Nevertheless, using acrylate adhesives may lead to problems related to the ductility of the connection and the consequent seismic resistance of the bearing elements, in addition to potential relative deformation of both connected materials under a strong temperature effect.

A fact that needs to be underlined is the existence of first timber buildings with HGV timber-glass elements (Austria) functioning as resisting wall elements under horizontal load and resisting the horizontal stiffening of the building. The most interesting is probably a low-energy two-storey single-family house in Eichgraben (Austria), Fig. 4.30. The timber frames of the wall elements were factory-made and transported to the building site where the glass elements were fixed to the timber frame using the HFA Pat.-Nr. 502470 type of connection [44].

The second building realized within the Holzforschung Austria (HFA) research project was a bungalow with a north-facing glass façade and a south-facing glass façade. The building revealed a feasible assembly and manufacture of the cladding system and offered open space for the future insights in durability and long-term behaviour of buildings [11]. As opposed to the family house in Eichgraben, the

Fig. 4.30 Two-storey single-family house with HGV wall elements, built in Eichgraben (Austria)

wall elements produced in a multi-panel timber-frame system were finalized in the factory and transported to the building site.

In the study by Blyberg [10], a shear wall element intended to be used as a load-bearing façade element was designed. The laminated-float-glass pane with a thickness of 10 mm was placed in the middle of the timber frame (Fig. 4.31). LVL (laminated veneer lumber) with a machined groove squared cross sections of 45 mm was used for timber elements. Timber was glued onto glass with the acrylate adhesive Sikafast and in a few cases, with the 2-component silicone-based adhesive Sikasil SG-500. The edge of the glass was thus visible. Three different load cases were used for both adhesive types; horizontal load, vertical load and a combination of horizontal and vertical loads. The elements were subjected to the horizontal point load and supported with two supports, the tensile and the compressive, in a similar way as in Neubauer and Schober [44] experiments.

The obtained maximal horizontal load for all tested elements was 41.4 kN for the silicone specimens and 67.8 kN for the acrylate specimens. While the results from the adhesive testing showed that the acrylate adhesive had much larger strength than the silicone adhesive, it should be noted that the acrylate has a glass-transition temperature of 52 °C, which could imply that the properties of the adhesive change at increased temperatures. It is also interesting to compare the results with the values obtained by Neubauer and Schober [44] tests. The reason for significantly higher lies in the fact that the bond line was only 1.5 mm thick, which is two times lower than in the case of the silicone type in Neubauer and Schober [44].

Fig. 4.31 Test configuration of the wall test specimens

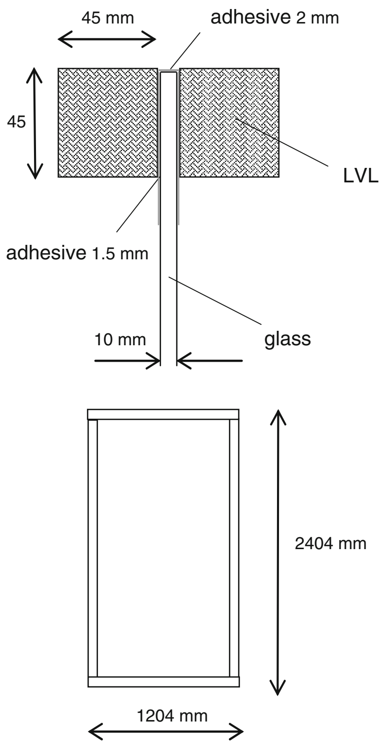

At the University of Minho, a new timber-glass panel element was developed which can be applied either as a slab (Fig. 4.32a) or a wall (Fig. 4.32b) prefabricated load-bearing element. According to its dimensional metrics, it is adjustable

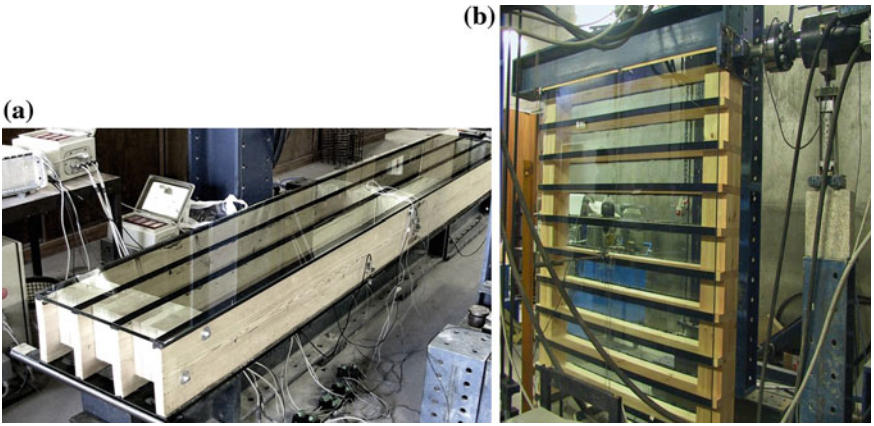

Fig. 4.32 Timber-glass panel **a** as a slab element [6], **b** as a wall element [48]

to several foreseen project situations. In the huge experimental analysis [6], twenty one panels were tested—eleven timber panels and ten timber-glass composite panels. Each composite panel was 224 mm thick and consisted of two laminated glass panes bonded on both faces of the timber structure, made of four Pinus Sylvestris timber boards, with a cross section of 200 mm x 30 mm. The specimens were tested in bending as slab elements and as wall elements subjected to vertical load.

The main conclusion to withdraw from this experimental work was that glass behaves as structural reinforcement of the timber substructure, particularly when used as a *structural slab element*, in which case the tests results showed excellent structural performance of the composite panel with an increase of 31 % in the maximum load obtained, in comparison with the glass-less panel.

As a *structural wall system* tested under vertical load, the contribution of glass became even more evident. The bearing capacity of the timber-glass composite panels was compared to that of timber panels without glass. The results showed a clear increase in the stiffness and resistance, which allowed the value of 100 kN to be exceeded, while still keeping a considerable safety margin and ductile failure at its post-high peak.

The following step was to develop several implantation models either as semi-detached houses or blocks in order to produce an innovative timber-glass composite construction system in which the combination of timber and glass simultaneously incorporates energetic, functional and aesthetic characteristics. Such system becomes an architectural and structural skin, a frontier between the inner and outer spaces reinforcing the importance of the structure's energetic performance and the comfort of its inhabitable space, predominantly in terms of thermal transfers, air circulation and natural lighting levels—features that definitely contribute to optimizing the energy efficiency and effectiveness of its management. The second phase involving optimization of the structural solution, based on the search for tectonics and a contemporary architectural system construction, led to the materialization of the housing model with the above-described load-bearing composite timber-glass slab and wall elements (Fig. 4.33).

A set of experimental tests on timber-frame-panel wall elements were also performed at the University of Maribor, in 2011 and 2012. The tests were subdivided into two main groups according to the position of the glass panes:

- Glass panes were placed on the external sides of the timber frame, Fig. 4.35 [49].
- A single glass pane was embedded into the middle plane of the timber frame, Fig. 4.38 [50].

The test specimens consisted of a timber frame with the outside edges measuring 1,250/2,640 mm (Fig. 4.35), which used to be a standard size of wall panels tested in previous studies where a different sheathing material was used, see Sects. 3.3 and 3.4. Vertical studs were composed of rectangular 90/90-mm timber elements with the size of horizontal girders being 90/80 mm. The bottom left-hand

Fig. 4.33 Application of prefabricated elements in a housing model [6]

corner of the panel had three 16-mm holes through which the panel was fixed into the stirrup functioning as the tensile support. Timber-frame elements in both cases were made of wood with a strength grade C22, glass panes consisted of toughened ESG glass, and the adhesive used in the timber-glass joint was a two-component silicone adhesive type Ködiglaze S, produced by Kömmerling [51]. In the second case, polyurethane and epoxy adhesives were additionally used. Material properties of timber with a strength grade C22 were taken from [52], with properties of thermally toughened glass being taken from [53] and [54] and those of adhesives obtained from the producer's technical sheet [55, 56]. All material properties are listed in Table 4.9.

Testing procedure

After a relaxation period of several days, the panels were installed in the static load testing machine. During the testing process, the panels were rotated by 90° and fixed with the left vertical stud via three coil bars Φ16 into the stirrup consisting of two steel plates, as shown in Fig. 4.34a. The reaction of the lower compression support was taken by the steel section I180, fixed to the stiff steel frame. The test specimens were exposed to force F which approximates lateral load, ranging from point 0 to the failure point according to the [57] static monotonic testing procedure, Fig. 4.34b. The load stress increase rate on the

Table 4.9 Properties of the materials used

	$E_{0,m}$ [N/mm^2]	G_m [N/mm^2]	$f_{t,0,k}$ [N/mm^2]	$f_{m,k}$ [N/mm^2]	$f_{v,k}$ [N/mm^2]
Timber C22	10,000.00	630	13.0	22.0	2.4
Thermally toughened glass EN 12150	70,000.00	28,000.00	45	120	/
2C Silicone adhesive (Ködiglaze S)	2.8	0.93	2.1	/	3.15
Polyurethane adhesive (Ködiglaze P)	1.0	0.33	2.0	/	2.0
Epoxy adhesive (Körapox 558)	26.0	8.58	28.59	/	22.0

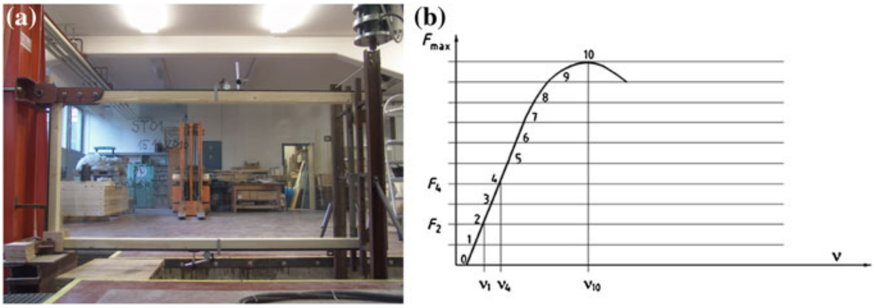

Fig. 4.34 Test configuration (**a**), and the load-testing procedure according to [57] (**b**)

panels was 2.0 kN/250 s for the values from 0 to 10 kN and 2.0 kN/200 s for the value of 10 kN to the point of failure.

4.4.1.1 Glass Panes Placed on the External Sides of the Timber Frame

The first step of the study involved glass panes with a thickness of 6 mm placed on the external sides of the timber frame. The type of connection resembled Joint 3 presented by Niedermaier [43], Fig. 4.27, but featured an important difference

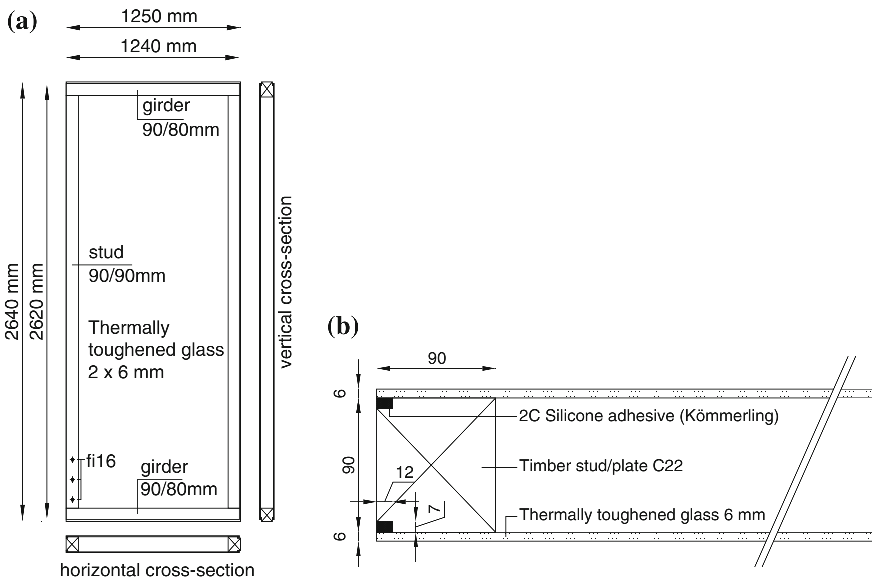

Fig. 4.35 Dimensions of the test specimens (**a**), and the section of the linear adhesive bonded joint (**b**)

Fig. 4.36 Brittle failure mode of the glass panes in compression

seen in the silicone adhesive being applied into a special groove in the timber frame (Fig. 4.35). The adhesive used had a thickness of 7 mm with the width of the glue line measuring 12 mm. An important part of the research focused on the impact of the relaxation time of the silicon adhesive, from the time of bonding to the starting point of the test specimen exposure to load. Consequently, the test specimens with the longest relaxation time ($t = 7$ days) were given the label ST-01, those with the shortest relaxation time ($t = 3$ days) were labelled as ST-02, and finally, the specimens with the middle relaxation time ($t = 5$ days) received the ST-03 label.

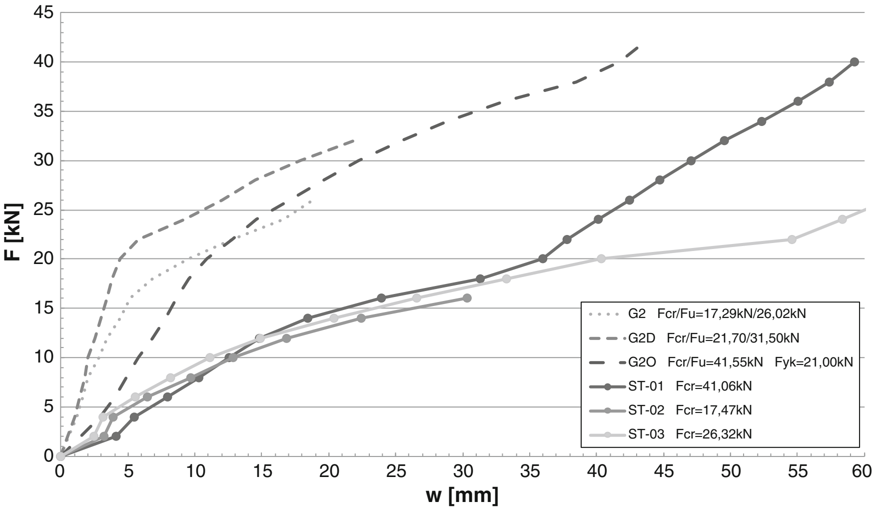

Fig. 4.37 F-w diagrams of the test specimens with different types of sheathing material [49]

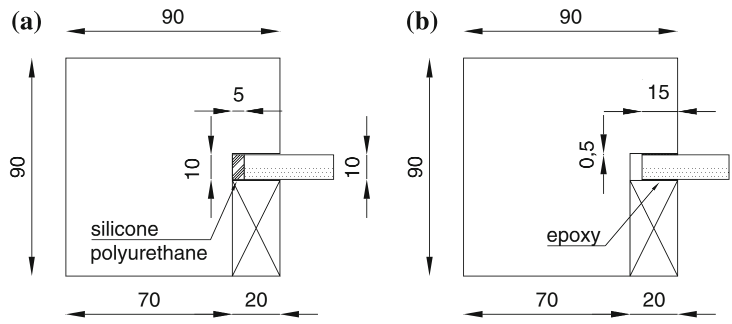

Fig. 4.38 Connection with a glue line in the middle of the timber frame **a** silicone and polyurethane adhesive, **b** epoxy adhesive

The behaviour of the tested samples was very similar and it proved a completely brittle failure mode of both external glass panes, occurring under the compressive stress in the glass pane, Fig. 4.36.

The results of all specimen groups are given in Fig. 4.37 which shows the normalized values of vertical displacements (w) relative to force F, separately for each specimen. The F_{cr} values given in the legend to the figure demonstrate the force at which the first crack appeared in the glass sheathing. Owing to the non-ductile behaviour of glass (Fig. 4.38), the latter force also meant the failure force. Figure 4.39 presents diagrams of the normalized mean values of displacements of

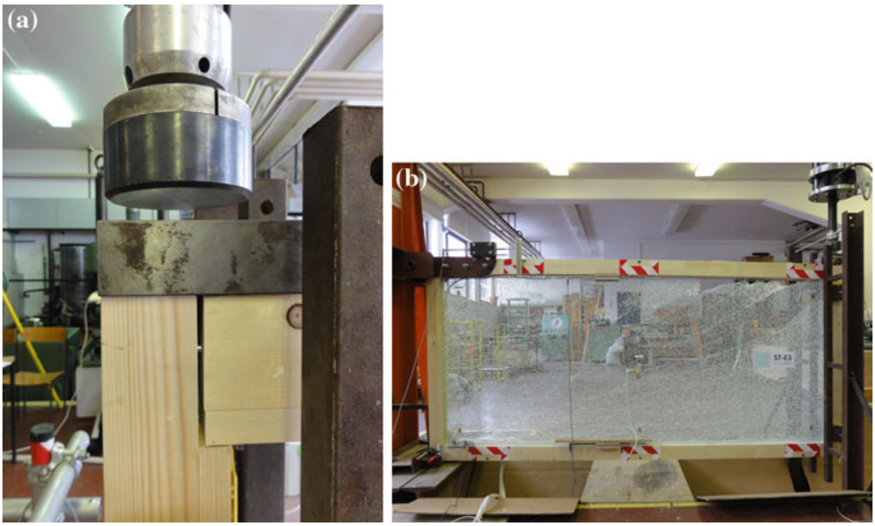

Fig. 4.39 Failure modes of the samples with a glass pane placed in the middle of the timber frame; **a** destruction of the timber corner in the case of using silicone and polyurethane adhesives, **b** a brittle glass rupture in the a case of epoxy adhesive

the test specimens, taken from our experimental study presented in Sects. 3.3 and 3.4, where the test specimens with identical geometrical characteristics as those in the present research had different sheathing materials. The glass panes are labelled as ST while the labels of other test specimens mean the following:

- G2—single FPB sheathing with a span of $s = 75$ mm between the staples
- G2D—double FPB sheathing with a span of $s = 75$ mm between the staples
- G2O—single OSB sheathing with a span of $s = 75$ mm between the staples.

The stiffness in the *F*-*w* diagram is defined by the inclination of the curve. The load-bearing capacity is defined by the value of the failure force.

The test specimen's behaviour demonstrated its dependence on the age of the silicone adhesive at the time of exposure to load. Subsequently, the behaviour of the test specimen ST-01 with the longest relaxation time ($t = 7$ days) proved to be the best and could be labelled as three-linear (phase 1: linear behaviour until the point of yielding of the adhesive; phase 2: yielding of the adhesive; phase 3: fixing in the connecting plane—the glass sheathing leans on the timber frame, which is followed by instantaneous failure of the glass sheathing). On the other hand, the test specimen ST-02 with the shortest relaxation time ($t = 3$ days) failed soon after the onset of the yielding of the adhesive.

Although the test specimen ST-01 can be compared to G20 in its load-bearing capacity, its stiffness is nevertheless essentially lower. A similar comparison of the load-bearing capacity can be made between the test specimens ST-03 and G2, where the latter displays approximately three times higher stiffness in the linear-elastic behaviour range. The above conclusions bear a close similarity to the findings presented by Niedermaier [43] Neubauer and Schober [44] and Cruz and Pequeno [6].

4.4.1.2 Single Glass Pane Embedded into the Middle Plane of the Timber Frame

Another possibility of using glass panes as a load-bearing sheathing material in timber-frame wall elements is to insert a single glass pane into the middle plane of the timber frame. A similar type of connection was already presented in the study by Niedermaier [43] (Fig. 4.27), Joint 1 and Joint 2. Our study comprised testing of three groups with different boundary conditions and adhesives:

- Silicone adhesive with a glue line thickness of 6 mm placed in the lateral plane of the connection (Fig. 4.38a).
- Polyurethane adhesive with a glue line thickness of 6 mm placed in the lateral plane of the connection (Fig. 4.38a).
- Epoxy adhesive with a glue line thickness of 0.5 mm placed in the shear plane of the connection (Fig. 4.38b).

Each test group consisted of three specimens. The aim of the study was to compare the results relative to application of different adhesives types, with a special focus on the obtained load-bearing capacity and stiffness after using an elastic adhesive (e.g., silicone) or a stiff adhesive like epoxy. Another point of analysis was the influence of the adhesive type on the ductility of the test samples. A single fully tempered (toughened) glass pane with a thickness of 10 mm having the material characteristics given in Table 4.9 was used for all test samples.

It is furthermore interesting to compare the behaviour of the tested samples with different boundary conditions and different types of the adhesives. The failure modes of the elements with elastic adhesives (silicone and polyurethane) demonstrated a relatively ductile failure with destruction of the corner connection between the timber elements (Fig. 4.39a). On the other hand, failure of the test samples with a very stiff adhesive (epoxy) was completely brittle with a glass rupture in the compressive diagonal (Fig. 4.39b). Both findings prove the Cruz et al. [7] conclusions.

Figure 4.40 presents diagrams of the normalized mean values of displacements of all tested samples with glass panes in addition to the results of the test specimens with identical geometrical characteristics but with different sheathing materials. The results obtained on silicone HGV test samples with the 14/3 mm (HGV 14/3) and 19/3 mm (HGV 19/3) glue lines, taken from Neubauer and Schober [44] and Hochhauser [45], merely serve to provide further comparison.

Similar results of the test samples with silicone and polyurethane adhesives prove to be an important piece of information relevant to a better overall technological advance of silicone adhesives, presented in Sect. 4.1. Silicone samples'

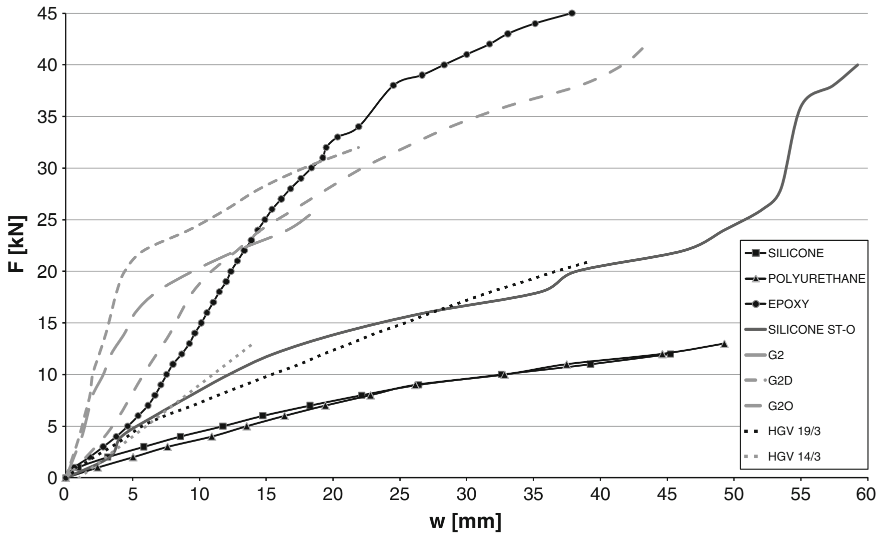

Fig. 4.40 F-w diagrams of the test specimens with different types of sheathing materials [50]

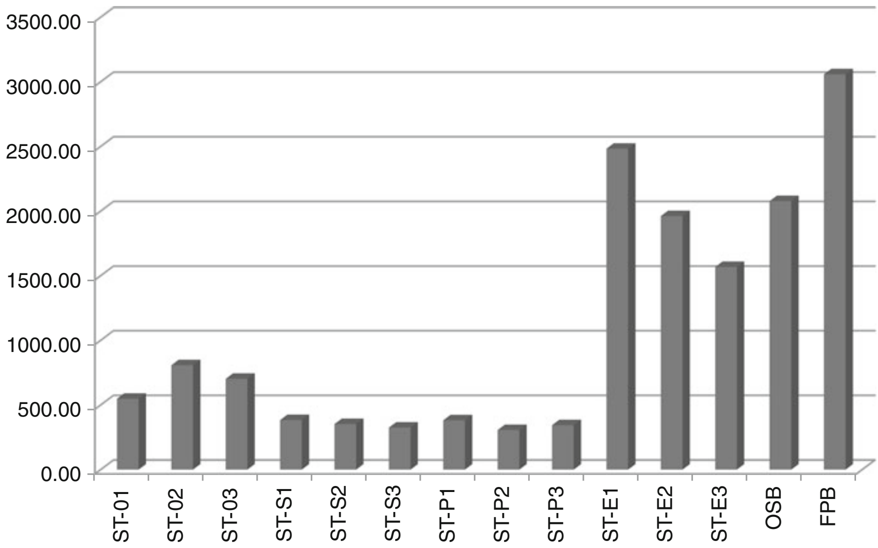

Fig. 4.41 Calculated results for the racking stiffness according to [57]

results are comparable to those by Neubauer and Schober [44] with a difference in the glue line dimensions being taken into account. Moreover, the failure force of the silicone and polyurethane test samples is set at about of 40–50 % of the values of typical classical sheathing materials (fibre-plaster boards or OSB). Nevertheless, a comparison with the results for the force forming the first crack (Table 3.12) in the fibre-plaster boards (F_{cr}) shows that the silicone adhesive specimens reached almost 70 % of the value obtained on the FBP test samples with a typical 75-mm span staple disposition. On the other hand, the results for the failure force of the epoxy adhesive test samples prove to be in an absolutely comparable range with those of the OSB boards.

As mentioned beforehand, the connection between glass and timber has the strongest influence on the stiffness of the wall elements, which is also evident from the results in Fig. 4.41 and from those for the racking stiffness (R) of all tested wall elements with glazing, calculated according to the [57] in the prescribed form of

$$R = \frac{F_4 - F_2}{w_4 - w_2} \tag{4.3}$$

and graphically presented in Fig. 4.41. The values for the elements with OSB and FPB boards are given for the purpose of the comparison of the stiffness.

The results of the mean values are found in Table 4.10.

The racking stiffness (R) for all glass test samples, with the exception of the epoxy type, was clearly far under the stiffness of the classical load-bearing wall elements with OSB or FPB sheathing boards. We can therefore point out once more that using glass elements instead of classical sheathing boards exerts a more

Table 4.10 Measured experimental results (mean values)

Type of the test samples	R [N/mm]	F_{cr} [kN]	F_y [kN]	$F_{u,k}$ [kN]
OSB 3 (s = 75 mm)	2,078.12	/	21.25	41.55
FPB (s = 75 mm)	3,059.39	17.06	/	26.17
ST-0 (silicone ext. side)	686.76	/	16.80	28.28
ST-S (silicone middle)	354.48	/	11.58	11.58
ST-P (polyureth. middle)	344.82	/	13.43	13.43
ST-E (epoxy middle)	2,004.41	37.35	/	37.35

F_{cr}— force forming the first crack in the sheathing board or glass pane
F_y—force forming the fasteners or adhesive yielding (or timber-frame corner destruction)
$F_{u,k}$— ultimate failure force (corner destruction or glass failure)

rigorous influence on the racking stiffness than on the load-bearing capacity of the wall elements, which consequently leads to more problems in satisfying the serviceability limit state requirements. The above findings are closely related to the conclusions drawn in Sect. 3.3.1, discussing the problem of non-resisting window and door openings in wall elements.

4.4.2 Computational Models

As presented in the experimental studies, there are many parameters which significantly influence the behaviour of timber-frame wall elements with glass panes exposed to horizontal load. The following are the most important:

- Type of glazing
- Thickness of the glazing
- Type of adhesive
- Dimensions of the glue line.

Designing timber-glass wall elements is thus a very complex process with the most important fact being the approximation of the timber-glass connection in the bond line. Since there is usually a shortage of time and funds to perform experimental analysis of the elements to be used, it is of utmost importance to develop appropriate computational models which will serve as means of accurate prediction of the horizontal load-bearing capacity and the horizontal stiffness of such wall elements. The models, based on general guidelines of designing timber-frame wall elements and already discussed in Sect. 3.3, can be classified in two main groups:

- Semi-analytical spring models
- Finite element models (FEM).

4.4.2.1 Semi-Analytical Spring Models

The models are based on the main assumptions relevant to the semi-analytical simplified composite beam model in Sect. 3.3.4. A major difference between the two types of models is replacing the timber-frame-sheathing board connection plane with the timber-glass bond line. It is consequently not possible to adopt the so-called γ-procedure used in the above-mentioned computational model to simulate the timber–board connection. The springs are used instead (Fig. 4.42).

The first of such static undetermined spring models was introduced by Kreuzinger and Niedermaier [58]. The timber-frame bending stiffness is supposed to be perfectly rigid (EI $= \infty$). Another approximation is identical stiffness of the springs longitudinal (k_u) and perpendicular (k_w) to the glue line ($k = k_u = k_w$). According to these simplifications and considering the classical beam theory, the maximal horizontal displacement (u) under the horizontal force (F_H) acting at the top of the wall element is developed in the form of:

$$u = \frac{2 \cdot F_H}{k \cdot b} \cdot \left(\frac{1}{1 + \frac{h}{3b}} + \frac{\frac{h}{b}}{1 + \frac{h}{3b}} \right) \tag{4.4}$$

In the above equation, the stiffness of the bond line (k) is determined in dependence on the shear modulus of the adhesive (G_{bl}), the thickness (d_{bl}) and the width (b_{bl}) of the bond line:

$$k = G_{bl} \cdot \frac{b_{bl}}{d_{bl}} \tag{4.5}$$

If we consider the shear stress (τ) as uniformly distributed along the bond line, then it can be written in the form of

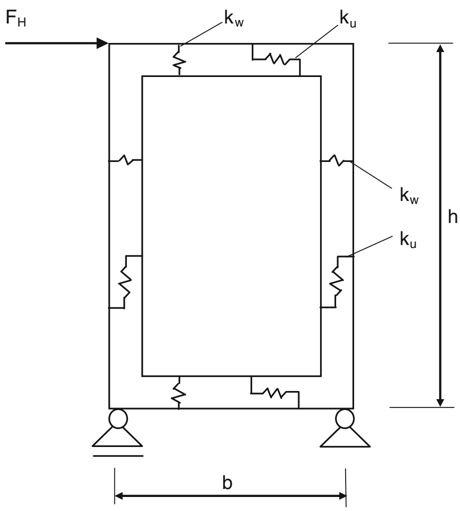

Fig. 4.42 Spring model introduced by Kreuzinger and Niedermaier [58]

$$\tau = \frac{F_H}{b_{bl} \cdot d_{bl}} \cdot \frac{1}{1 + \frac{h}{3b}} \tag{4.6}$$

and the slip (Δ) in the bond line between the glass pane and timber-frame elements can be finally developed in the form of

$$\Delta = \frac{\tau}{G_{bl}} \cdot d_{bl} \tag{4.7}$$

4.4.2.2 Finite Element Models

The process of modelling timber-frame wall elements with glass panes under the horizontal load by using the Finite Element Method is the most accurate but at the same time the most complex and time-consuming approach. In view of the latter, simplified "hand-calculating" methods described beforehand tend to be applied in practice since they provide the user with results without recourse to complex and expensive software.

FEM modelling of the timber-glass composite wall elements is based on the process of modelling timber-frame wall elements with classical sheathing boards (FPB or OSB) with and without openings (c.f. Sect. 3.3.1), schematically presented in Fig. 3.4. *Timber-frame material* is considered as an isotropic elastic material, and the elements of the timber frame are modelled as simple plane-stress elements. The *glass panes* are modelled by using the non-linear 2D shell elements. Since the material behaviour of glass proves to be extremely non-ductile with brittle failure modes, glass is presumed to be linear-elastic until failure. The *bond line* between timber and glass is modelled with 3D layer elements having the material characteristics of the adhesive.

References

1. Rasmussen SC (2012) How glass changed the world, the history and chemistry of glass from antiquity to the 13th century. Springer
2. Staib G (1999) From the origins to classical modernism. In: glass construction manual. Birkhäuser—Publishers for Architecture
3. Wurm J (2007) Glass structures—design and construction of self-supporting skins. Birkhäuser Verlag AG, Basel, Boston, Berlin
4. Močibob D (2008) Glass panel under shear loading—use of glass envelopes in building stabilization. PhD thesis, EPFL, Thèse no 4185, Lausanne, Switzerland
5. Balkow D (1999) Glass as a building material. In: glass construction manual. Birkhäuser—publishers for architecture
6. Cruz P, Pequeno J (2008) Timber-glass composite structural panels: experimental studies and architectural applications. Conference on architectural and structural applications of glass, Delft University of Technology, Faculty of Architecture, Delf, Netherlands

7. Cruz P, Pacheco J, Pequeno J (2007) Experimental studies on structural timber glass adhesive bonding. COST E34, bonding of timber, 4th workshop ≫ practical solutions for furniture and structural bonding, Golden Bay Beach Hotel, Larnaca, Cyprus, 22–23 Mar 2007
8. Haldimann M, Luible A, Overend M (2008) Structural use of glass. IABSE 2008
9. Blyberg L, Serrano E, Enquist B, Sterley M (2012) Adhesive joints for structural timber/glass applications: experimental testing and evaluation methods. Int J Adhes Adhes 35:76–87
10. Blyberg L (2011) Timber/glass adhesive bonds for structural applications. Licentiate thesis by Louise Blyberg, Linnaeus University, School of Engineering
11. Winter W, Hochhauser W, Kreher K (2010) Load bearing and stiffening timber-glass-composites (TGC). WCTE 2010 conference proceedings
12. Pequeno J, Cruz P (2009) Structural timber-glass linear system: characterization and architectural potentialities. Glass performance days 2009, Tampere, Finland
13. UNIGLAS® (2010) College technical compendium, 1st ed., UNIGLAS® GmbH & Co. KG, Montabaur
14. ISO 10077-1:2006 (2006) Thermal performance of windows, doors and shutters. Calculation of thermal transmittance
15. Dow corning insulating glass manual', literature number 62-1374D-01
16. Gustavsen A, Jelle BP, Arasteh D, Kohler K (2007) State-of-the-art highly insulating window frames. Research and market review, Oslo
17. Johnson R, Sullivan R, Selkowitz S, Nozaki S, Conner C, Arasteh D (1984) Glazing energy performance and design optimization with daylighting. Energy Build 6:305–317
18. Steadman P, Brown F (1987) Estimating the exposed surface area of the domestic stock. Energy and urban built form, Centre for Architectural and Urban Studies, University of Cambridge, pp 113–131
19. Inanici NM, Demirbilek FN (2000) Thermal performance optimization of building aspect ratio and south window size in five cities having different climatic characteristic of Turkey. Build Environ 35(1):41–52
20. Bülow-Hübe H (2001) The effect of glazing type and size on annual heating and cooling demand for Swedish offices. (Report No TABK–01/1022). Department of construction and architecture, Lund University, Division of Energy and Building Design, Lund
21. Persson ML, Roos A, Wall M (2006) Influence of window size on the energy balance of low energy houses. Energy Build 38:181–188
22. Persson ML (2006) Windows of opportunities, the glazed area and its impact on the energy balance of buildings. PhD Thesis, Uppsala Universitet
23. Ford B, Schiano-Phan R, Zhongcheng D (2007) The passivhaus standard in European warm climates, design guidelines for comfortable low energy homes—part 2 and 3. Passive-on project report. School of the built environment, University of Nottingham
24. Bouden C (2007) Influence of glass curtain walls on the building thermal energy consumption under Tunisian climatic conditions: the case of administrative buildings. Renew Energy 32:141–156
25. Hassouneh K, Alshboul A, Al-Salaymeh A (2010) Influence of windows on the energy balance of apartment buildings in Amman. Energy Convers Manage 51:1583–1591
26. Praznik M, Kovič S (2010) With active systems and thermal protection to passive and plus energy residential buildings. Published international conference proceedings, energy efficiency in architecture and civil engineering, University of Maribor, Faculty of civil engineering, Maribor, pp 45–57
27. Žegarac Leskovar V, Premrov M (2011) An approach in architectural design of energy-efficient timber buildings with a focus on the optimal glazing size in the south-oriented Façade. Energy Build 43:3410–3418
28. Žegarac Leskovar V (2011) Development of design approach for the optimal model of an energy-efficient timber house. PhD Thesis, Graz University of Technology
29. ARSO (2010) Climate conditions in Slovenia. http://meteo.arso.gov.si/uploads/probase/www/climate/text/sl/publications/podnebne_razmerev_Sloveniji_71_00.pdf, (20.08.2010)
30. Feist V (2007) PHPP 2007 guide book. Passivhaus Institut Dr. Wolfgang Feist Darmstadt

31. Al Anzi A, Seo D, Krarti M (2009) Impact of building shape on thermal performance of office buildings in Kuwait. Energy Convers Manage 50(3):822–828
32. Depecker P, Menezo C, Virgone J, Lepers S (2001) Design of building shape and energetic consumption. Build Environ 36(5):627–635
33. Albatici R, Passerini F (2011) Bioclimatic design of buildings considering heating requirements in Italian climatic conditions. A simplified approach. Build Environ 46(8):1624–1631
34. Chiras D (2002) The solar house: passive heating and cooling. Chelsea Green Publishing, White River Junction
35. Hachem C, Athienitis A, Fazio P (2011) Parametric investigation of geometric form effects on solar potential of housing units. Sol Energy 85:1864–1877
36. Ecotect analysis (2011) Sustainable building design software—Autodesk
37. Hoadley RB (2000) Understanding wood, A Crafstman‘s guide to wood technology. The Taunton Press, USA
38. Luible A (2004) Stabilität von Tragelementen aus Glas. PhD thesis, EPFL, Thèseno 3014, Lausanne, Switzerland
39. Wellershoff F (2006) Nutzung der Verglasung zur Aussteifung von Gebäudehüllen. PhD Thesis, Schriftenreihe—Stahlbau RWTH Aachen, Heft 57, Shaker Verlag, Aachen, Germany
40. Weller B (2007) Designing of bonded joints in glass structures. In: Proceedings of the 10th international conference on architectural and automotive glass (GPD), Tampere, Finland, pp 74–76
41. Schober KP, Leitl D, Edl T (2006) Holz-Glas-Verbundkonstruktionen zur Gebäudeaussteifung. Magazin für den Holzbereich, Heft 1, Holzforschung Austria, Vienna
42. Huveners EMP (2009) Circumferentially adhesive bonded glass panes for bracing steel frames in facades. PhD thesis, University of Technology Eindhoven, Netherland
43. Niedermaier P (2003) Shear-strength of glass panel elements in combination with timber frame constructions. In: Proceedings of the 8th international conference on architectural and automotive glass (GPD), Tampere, Finland, pp 262–264
44. Neubauer G, Schober KP (2008) Holz-Glas-Verbundkonstruktionen, Weiterentwicklung und Herstellung von Holz-Glas-Verbundkonstruktionen durch statisch wirksames Verkleben von Holz und Glas zum Praxiseinsatz im Holzhausbau (Impulsprojekt V2 des Kind Holztechnologie), Endbericht, Holzforschung Austria, Vienna, Austria
45. Hochhauser W (2011) A contribution to the calculation and sizing of gued and embedded timber-glass composite panes. PhD Thesis, Vienna University of Technology, Faculty of Civil Engineering, Austria
46. Hochhauser W, Winter W, Kreher K (2011) Holz-Glas-Verbundkonstruktionen—state of the art, Forschungsbericht, Studentische Arbeiten. Technische Universitat Wien, Institut fur Architekturwissenschaften Tragwerksplanung und Ingenieurholzbau
47. European committee for standardization (1996) EN 594:1996: timber structures—test methods—racking strength and stiffness of timber frame wall panels. Brussels
48. Cruz P, Pequeno J, Lebet JP, Mocibob D (2010) Mechanical modelling of in-plane loaded glass panes. Challenging glass 2—conference on architectural and structural applications of glass, TU Delft, May 2010
49. Ber B, Kuhta M, Premrov M (2011) Glazing influence on the horizontal load capacity and stiffness of timber-framed walls. In: Proceedings of the 33rd assembly of structural engineers of Slovenia, Bled, 6–7 Oct 2011, pp 301–308
50. Ber B, Premrov M, Kuhta M (2012) Horizontal load-carrying capacity of timber-framed walls with glass sheathing in prefabricated timber construction. In: Proceedings of the 34th assembly of structural engineers of Slovenia, Bled, 11–12 Oct 2012, pp 211–218
51. Kömmerling (2008) Product information Ködiglaze S—special adhesive for structural and direct glazing
52. European committee for standardization (2003) EN 338:2003 E: structural timber—strength classes. Brussels

53. Kömmerling (2008) Product information Ködiglaze P—special adhesive for bonding insulating glass units into the window sash
54. European committee for standardization (2004) EN 572-1:2004: glass in building—basic soda lime silicate glass products—part 1: definitions and general physical and mechanical properties. Brussels
55. European committee for standardization (2000) EN 12150-1:2000: glass in building—thermally toughened soda lime silicate safety glass—part 1: definition and description. Brussels
56. Kömmerling (2011) Product information Körapox 558—two component reaction adhesive for bonding of metals, for example steel or aluminium to each other
57. European committee for standardization (2011) EN 594:2011: timber structures—test methods—racking strength and stiffness of timber frame wall panels. Brussels
58. Kreuzinger H, Niedermaier P (2005) Glas als Schubfeld. Tagungsband Ingenieurholzbau, Karlsruher Tage
59. European Committee for Standardization CEN/TC 250/SC5 N173 (2005) EN 1995-1-1:2005 Eurocode 5: design of timber structures, part 1-1 general rules and rules for buildings, Brussels
60. CSN EN 1279-1—glass in building—insulating glass units—part 1: generalities, dimensional tolerances and rules for the system description